Probabilistic Engineering Mechanics 39 (2015) 23–38

Contents lists available at ScienceDirect

Probabilistic Engineering Mechanics

journal homepage: www.elsevier.com/locate/probengmech

Dynamic analysis of stochastic structural systems using frequency adaptive spectral functions

A. Kundu, S. Adhikari *

College of Engineering, Swansea University, Singleton Park, Swansea SA2 8PP, UK

ARTICLE INFO

Article history:
Received 28 October 2014
Accepted 17 November 2014
Available online 29 November 2014

Keywords:
Stochastic structural dynamics
KL expansion
Spectral functions
Stochastic projection
Frequency response
Damped vibration

ABSTRACT

A novel Galerkin subspace projection scheme for linear structural dynamic systems with stochastic coefficients is developed in this paper. The fundamental idea is to solve a discretized stochastic system in the frequency domain by projecting the solution on a reduced subspace of eigenvectors of the deterministic operator weighted by a set of frequency dependent stochastic functions, termed as the spectral functions. These spectral functions are rational functions of the input random variables and a study of the different orders of spectral functions are presented. A set of undetermined Galerkin coefficients are utilized to orthogonalize the residual to the reduced eigenvector space in the mean sense. The complex system response is represented explicitly with these Galerkin coefficients in conjunction with the modal basis and the associated stochastic spectral functions. The statistical moments of the solution are evaluated at all frequencies and the solution accuracy is verified in terms of a relative error norm. Two examples involving a beam and a plate with stochastic parameters subjected to harmonic excitations have been studied. The results are compared with the direct Monte-Carlo simulation, the classical Neumann expansion technique and the polynomial chaos method for different orders stochastic functions and varying degrees of variability of input randomness.

1. Introduction

Computational models of physical systems often use idealized approximations, such as in parameter values and boundary conditions, which cannot be known for certain. This has led to investigation into stochastic computer models which incorporate probabilistic description of the uncertain quantities into the model (such as [1–3]). In this study we concentrate on the frequency domain response of damped structural dynamic systems with parametric uncertainty which is multiplicative in nature. The objective is to propose a novel uncertainty propagation scheme for probabilistic inputs to the structural dynamic model (as parametric uncertainty) and investigate the accuracy, convergence and computational cost of the proposed method. There are two broad classes of the uncertainty propagation techniques for the stochastic systems – statistical sample based simulations and the non-statistical analytical methods.

Various Monte Carlo Simulation (MCS) techniques belong to the class of non-intrusive sample based methods and have been used in context of the structural dynamics problems [4]. The slow convergence rate of MCS makes it unfeasible for practical implementation and various improved sampling techniques such as the importance sampling, Latin hypercube sampling, have been proposed which can be regarded as the "variance reduction techniques" [5]. The limitations of these techniques are dictated by the dimension of the stochastic space. Uncertain structural systems represented by few random variables subjected to deterministic loading can be well-suited for such variance reduction procedures [6].

The alternatives to the sampling techniques provide an explicit functional relationship between the input random variables which allows easy evaluation of the functional statistics. Such solvers include perturbation method [7], or equivalently the lower-order Taylor approximation and the Neumann expansion method, [8,9] all of which comes down to the estimation of response surface in a parameter space. On the other hand the stochastic Galerkin methods [10–12] allows the response to be expressed with orthogonal basis functions spanning the stochastic space. The accurate estimation of the high order statistical moments, or the full probability distribution function, of the response requires high degree polynomials, which in turn results in high dimensional block sparse linear system of equations. Krylov-type iterative techniques have been proposed to solve such systems efficiently by exploiting the sparsity of the system [13,14]. However, the difficulty to build efficient preconditioners and the memory

* Corresponding author. Fax: +44 1792 295676.
E-mail addresses: a.kundu@swansea.ac.uk (A. Kundu), S.Adhikari@swansea.ac.uk (S. Adhikari).

http://dx.doi.org/10.1016/j.probengmech.2014.11.003
0266-8920/

requirements induced by these techniques are still challenging and active areas of research.

We consider a bounded domain $\mathcal{D} \in \mathbb{R}^d$ with piecewise Lipschitz boundary $\partial\mathcal{D}$, $d \leq 3$ is the spatial dimension and $t \in \mathbb{R}^+$ is the time. We take $(\Theta, \mathcal{F}, P)$ as the probability space where $\theta \in \Theta$ is a sample point from the sampling space Θ, $\mathcal{F}$ is the complete Borel σ-algebra over the subsets of Θ and P is the probability measure. We consider here the linear stochastic partial differential equation (pde) for elastodynamic systems with parametric uncertainty:

$$\rho(\mathbf{r},\theta)\frac{\partial^2 u(\mathbf{r},t,\theta)}{\partial t^2} + \mathfrak{L}_{\mathbf{c}}\frac{\partial u(\mathbf{r},t,\theta)}{\partial t} + div(\sigma_\alpha(u(\mathbf{r},t,\theta))) = p(\mathbf{r},t); \quad \mathbf{r}\in\mathcal{D},\ t\in[0,T],\ \theta\in\Theta \tag{1}$$

with the associated Dirichlet condition $u(\mathbf{r},t,\theta)=0$; $\mathbf{r}$ on $\partial\mathcal{D}$. Here $\sigma_\alpha(u(\mathbf{r},t,\theta))$ is the stress tensor with stiffness coefficient $\alpha(\mathbf{r},\theta)$ modeled as a stationary, square integrable random field such that α: $\mathbb{R}^d \times \Theta \to \mathbb{R}$. The operator $div(\sigma_a)$ is taken to be a self-adjoint stochastic stiffness operator. $\mathfrak{L}_{\mathbf{c}}$ is the damping operator containing the stochastic coefficient vector $\mathbf{c}(\mathbf{r},\theta)$. The damping operator along with its coefficients can be utilized to represent various damping models like the strain rate dependent viscous damping or the velocity dependent viscous damping. $p(\mathbf{r},t)$ is the deterministic excitation field for which the solution $u(\mathbf{r},t,\theta)$ is sought. To perform harmonic analysis, Eq. (1) is transformed to the frequency domain as

$$-\omega^2\rho(\mathbf{r},\theta)\tilde{u}(\mathbf{r},\omega,\theta) + i\omega\mathfrak{L}_{\mathbf{c}}\tilde{u}(\mathbf{r},\omega,\theta) + div\left(\sigma_\alpha(\tilde{u}(\mathbf{r},\omega,\theta))\right) = \tilde{p}(\mathbf{r},\omega); \quad \omega\in\Omega \tag{2}$$

where Ω denotes the frequency space of the problem, with $\tilde{p}$ and $\tilde{u}$ representing the complex harmonic amplitudes. $\mathbf{E}(\alpha)$ in the stress–strain relationship $\sigma_\alpha = \mathbf{E}(\alpha)$: ε is the symmetric positive definite elasticity tensor which depends on the scalar random parameter α with ε being the strain tensor expressed as $\varepsilon = \mathbf{D}\tilde{\mathbf{u}}$. Well established techniques of variational formulation of the displacement-based deterministic finite-element methods [7,15] gives the following bilinear form for the elastodynamic system:

$$\mathcal{B}(\tilde{\mathbf{v}},\tilde{\mathbf{u}};\theta) = -\omega^2\int_{\mathcal{D}}\tilde{\mathbf{v}}\rho(\mathbf{r},\theta)\tilde{\mathbf{u}}\,d\mathcal{D} + i\omega\int_{\mathcal{D}}\tilde{\mathbf{v}}\mathfrak{L}_{\mathbf{c}}\tilde{\mathbf{u}}\,d\mathcal{D} + \int_{\mathcal{D}}\{\mathbf{D}\tilde{\mathbf{v}}\}^T\mathbf{E}(\alpha)\left\{\mathbf{D}\tilde{\mathbf{u}}\right\}d\mathcal{D} \tag{3}$$

$$\mathcal{L}(\tilde{\mathbf{v}};\theta) = \int_{\mathcal{D}}\tilde{\mathbf{v}}\tilde{p}\,d\mathcal{D}$$

$$\text{so that,}\quad \mathcal{B}(\tilde{\mathbf{v}},\tilde{\mathbf{u}};\theta) = \mathcal{L}(\tilde{\mathbf{v}};\theta) \qquad \forall\ \tilde{\mathbf{v}}\in\mathcal{E}[\mathcal{D}] \tag{4}$$

where $\mathcal{E}[\mathcal{D}]$ is the space of admissible trial functions which have finite strain energy on the spatial domain and satisfying the prescribed boundary conditions. Eq. (4) gives a set of discretized linear algebraic equations in terms of the mass, damping and stiffness matrices. These can be expressed in a compact form as

$$\mathbf{A}(\omega,\theta)\tilde{\mathbf{u}}(\omega,\theta) = \tilde{\mathbf{p}}(\omega); \quad \forall\ \theta\in\Theta;\ \omega\in\Omega;\ \mathbf{A}\in\mathbb{C}^{n\times n};\ \tilde{\mathbf{u}},\tilde{\mathbf{p}}\in\mathbb{C}^n \tag{5}$$

where $\mathbf{A}(\omega,\theta)$ is the complex frequency dependent coefficient matrix which inherits the uncertainty of the random parameters involved in the governing pde. The detailed description of these matrices is given in Section 3.1.

The paper has been arranged as follows. In Section 2 a brief overview of the stochastic finite element method is presented. The spectral decomposition technique in space of eigen vectors adopted in this study is detailed in Section 3 along with a description of the spectral functions proposed here. In Section 4 a redu ced Galerkin error minimization approach is proposed. The post-processing of the results to obtain the response moments are discussed in Section 5. Based on the theoretical results, a simple computational approach is shown in Section 6 where the proposed method of reduced spectral basis is applied to the stochastic dynamical system of an one-dimensional Euler–Bernoulli beam and a two-dimensional Kirchhoff–Love thin plate. A summary of the results and major conclusions arising from this study are given in Section 7.

2. Brief review of the stochastic finite element method

2.1. Discretization of random fields

The parametric uncertainty is generally associated with a covariance function $cov[a]$: $\mathcal{D}\times\mathcal{D}\to\mathbb{R}$ defined on the open, bounded polygonal domain in $\mathcal{D}$. For second order random fields, there is a compact self-adjoint operator:

$$T_a v(\cdot) = \int_{\mathcal{D}} cov[a](\mathbf{r},\cdot)v(\mathbf{r})d\mathbf{r} \quad \forall\ v\in L^2(\mathcal{D}) \tag{6}$$

along with a sequence of non-negative eigenpairs $\{(\lambda_i,\varphi_i)\}_{i=1}^{\infty}$ which describes the eigenvalue problem as

$$T_a\varphi_i = \lambda_i\varphi_i, \quad (\varphi_i,\varphi_j)_{L^2(\mathcal{D})} = \delta_{ij} \tag{7}$$

The truncated Karhunen–Loève (KL) expansion of the stochastic process $a(\mathbf{r},\theta)$ using these eigen-functions is expressed as

$$\hat{a}_m(\theta,\mathbf{r}) = E[a](\mathbf{r}) + \sum_{i=1}^{m}\sqrt{\lambda_i}\varphi_i(\mathbf{r})\xi_i(\theta) \quad \forall\ m\in\mathbb{N}_+ \tag{8}$$

where $E[a](\mathbf{r})$ is the mean function, $\{\xi_i(\theta)\}_{i=1}^m$ are a set of mutually independent, uncorrelated standard Gaussian random variables with zero mean ($E(\xi_i)=0$) and unit variance ($E(\xi_i^2)=1$). The eigenfunctions $\varphi_i(\mathbf{r})$ can be assumed to have sufficient smoothness for smooth covariance functions, and if the eigenpairs are decaying according to at least $\sqrt{\lambda_k}\,\|\varphi_k\|_{L^\infty(\mathcal{D})} = O(1/(1+k^s))$ for some decay exponent $s>1$, then $\|a-\hat{a}_m\|_{L^\infty(\mathcal{D})}\to 0$, [11]. For practical engineering problems, the parametric randomness is modeled with a finite set of random variables $\boldsymbol{\xi} = (\xi_1,\xi_2,\ldots,\xi_m)$: $\Theta\to\mathbb{R}^m$, using first few largest eigenpairs in the reduced probability space [16].

For arbitrary random field models, the random parameter can be expressed in a mean-square convergent series using a finite order chaos-expansion in terms of the basic independent identically distributed (iid) random variables $\hat{\boldsymbol{\xi}}(\theta) = \{\hat{\xi}^{(1)},\ldots,\hat{\xi}^{(n)}\}$ as $a(\mathbf{r},\theta) = \sum_{i=0}^{p}\mathcal{H}_i(\hat{\boldsymbol{\xi}}(\theta))a_i(\mathbf{r})$ where $\mathcal{H}_i(\hat{\boldsymbol{\xi}}(\theta))$ are the multivariate orthogonal polynomial functions depending on the joint probability density function of the stochastic Hilbert space. The solution methodology presented in this paper is applicable to this kind of general decomposition of the random field.

2.2. Spectral methods and other solution techniques

The spatially discretized solution vector $\tilde{\mathbf{u}}(\omega,\theta)$ lies in the tensor product space $\mathbb{C}^n\otimes\Upsilon$, where Υ is an ad-hoc function space for real-valued random variables [10]. Since the stochastic system is represented with finite set of iid random variables $\hat{\boldsymbol{\xi}}(\theta) = \{\hat{\xi}^{(1)},\ldots,\hat{\xi}^{(p)}\}$ as in Section 2.1, the stochastic space is given as $\Upsilon_p\subset\Upsilon$. Given that each random component $\hat{\xi}^{(i)}$ is independent, Υ_p is of the tensor product form $\Upsilon^1\otimes\Upsilon^2\otimes\ldots\otimes\Upsilon^p$. The solution vector in Eq. (5) can be expressed in the form:

$$\tilde{\mathbf{u}}(\omega,\theta) = \sum_{\alpha\in\mathcal{I}_p}\mathcal{H}_\alpha(\omega,\theta)\tilde{u}_\alpha(\omega); \quad \tilde{u}_\alpha(\omega)\in\mathbb{C}^n \tag{9}$$

where $\mathcal{H}_\alpha$ are the bases in Υ_p ($\mathcal{I}_p$ being the cardinality of the set consisting of $\mathcal{H}_\alpha$) and $\tilde{u}_\alpha(\omega)$ are the set of unknown coefficients to be evaluated. It is evident from the above steps that the approximate basis functions can be chosen to depend on frequency which can allow for the efficiency of the solution technique to be frequency adaptive and hence well suited for applications over a wide frequency range.

The form of the stochastic bases $\mathcal{H}_\alpha(\omega, \theta)$ in Eq. (9) varies according to the chosen solution approach. The stochastic Galerkin approaches use orthogonal polynomial bases $\mathcal{H}_\alpha(\theta)$ [17]. Thus the stochastic spectral Galerkin method poses the problem as it is necessary to find $\tilde{u}_\alpha(\omega) \in \mathbb{C}^n \otimes \Upsilon_p$ such that

$$\sum_{\alpha \in \mathcal{I}_p} \mathbb{E}(\mathbf{A}\mathcal{H}_\beta \mathcal{H}_\alpha)\tilde{u}_\alpha = \mathbb{E}(\mathcal{H}_\beta \tilde{\mathbf{p}}) \quad \forall\, \beta \in \mathcal{I}_p \tag{10}$$

which gives a set of linear algebraic equations. Frequency domain analysis of stochastic systems has been studied using this method [18] for the medium-frequency structural dynamic analysis. However, the computational cost associated with the inversion of the coefficient matrix in Eq. (10) can become prohibitive for systems with large dimensions and near resonance frequencies even for moderate values of variability of the input random field. Preconditioning can often improve the efficiency of the linear system solver, but the availability of optimal pre-conditioners is often limited to systems with low variance.

3. Projection of stochastic dynamic response in the modal space

3.1. Finite element modeling of structural dynamic systems

Using the discretized random field model illustrated in Section 2.1, the stochastic system matrices can be derived from Eq. (1) using the well-established standard methods found in the stochastic FEM literature [19,11,12]. Following those developments, the stochastic PDE along with the boundary conditions would result in a set of equations in the frequency domain as

$$[-\omega^2\mathbf{M}(\theta) + i\omega\mathbf{C}(\theta) + \mathbf{K}(\theta)]\tilde{\mathbf{u}}(\omega, \theta) = \tilde{\mathbf{f}}_0(\omega) \tag{11}$$

where $\mathbf{M}(\theta) = \mathbf{M}_0 + \sum_{i=1}^{p_1} \mu_i(\theta_i)\mathbf{M}_i \in \mathbb{R}^{n\times n}$ is the random mass matrix, $\mathbf{K}(\theta) = \mathbf{K}_0 + \sum_{i=1}^{p_2} \nu_i(\theta_i)\mathbf{K}_i \in \mathbb{R}^{n\times n}$ is the random stiffness matrix along with $\mathbf{C}(\theta) \in \mathbb{R}^{n\times n}$ the random damping matrix. Here ($\mathbf{M}_0$ and $\mathbf{K}_0$) are the deterministic components while ($\mathbf{M}_i$ and $\mathbf{K}_i$) are the random contributions. The random mass and the stiffness matrices have been modeled with p_1 and p_2 random variables respectively. In the present work proportional damping is considered for which $\mathbf{C}(\theta) = \zeta_1\mathbf{M}(\theta) + \zeta_2\mathbf{K}(\theta)$, where ζ_1 and ζ_2 are deterministic scalars. $\tilde{\mathbf{u}}(\omega, \theta)$ is the complex frequency domain system response amplitude, $\tilde{\mathbf{f}}_0(\omega)$ is the amplitude of the harmonic force and ω is the frequency.

The random variables associated with the mass and stiffness matrices are grouped as $\xi_i(\theta) = \mu_i(\theta)$ for $i = 1, \ldots, p_1$ and $\xi_j(\theta) = \nu_{j-p_1}(\theta)$ for $j = p_1 + 1, \ldots, p_1 + p_2$. The linear structural system in Eq. (11) can then be expressed as

$$\left(\mathbf{A}_0(\omega) + \sum_{i=1}^{M} \xi_i(\theta)\mathbf{A}_i(\omega)\right)\tilde{\mathbf{u}}(\omega, \theta) = \tilde{\mathbf{f}}_0(\omega) \tag{12}$$

where $\mathbf{A}_0 \in \mathbb{C}^{n\times n}$ and $\mathbf{A}_i \in \mathbb{C}^{n\times n}$ represent the complex deterministic and stochastic parts of the system matrix and $M = p_1 + p_2$ is the total number of random variables used to represent the input random parameters. The expressions for $\mathbf{A}_0$ and $\mathbf{A}_i$ vary according to the damping model chosen for a particular application. For the case of proportional damping, the matrices $\mathbf{A}_0$ and $\mathbf{A}_i$ are given as

$$\mathbf{A}_0(\omega) = [-\omega^2 + i\omega\zeta_1]\mathbf{M}_0 + [i\omega\zeta_2 + 1]\mathbf{K}_0 \tag{13}$$

$$\text{and} \quad \mathbf{A}_i(\omega) = [-\omega^2 + i\omega\zeta_1]\mathbf{M}_i \quad \text{for } i = 1, 2, \ldots, p_1$$
$$\mathbf{A}_j(\omega) = [i\omega\zeta_2 + 1]\mathbf{K}_j \quad \text{for } j = p_1 + 1, p_1 + 2, \ldots, p_1 + p_2 \tag{14}$$

Eq. (12) together with the above equations completely define the discretized system considered in this study. Here $\mathbf{A}_0(\omega)$ and $\mathbf{A}_i(\omega) \in \mathbb{C}^{n\times n}$; $i = 1, 2, \ldots, M$ are complex symmetric frequency dependent matrices. The aim of this study is to efficiently obtain $\mathbf{u}(\omega, \theta)$ for $\theta \in \Theta$ and for all frequency values ω.

3.2. Derivation of the frequency-dependent spectral functions

An approximation to the solution of Eq. (12) can be construed as a linear combination of stochastic functions weighted with deterministic vectors which has been studied previously in context of statical systems in [20]. We extend that to the study of dynamical systems here using a reduced order stochastic approximation in conjunction with a Galerkin approach. A hybridization of the stochastic spectral function method with the Bayesian metamodeling approach has been studied in [21] to mitigate the computational cost of evaluation of the expensive high order stochastic functions. The present work is concerned with the detailed investigation of the properties of spectral functions in stochastic structural dynamic systems and the accuracy of the approximated response. The interpretation of spectral functions as the stochastic modal contribution factors, their property of frequency adaptivity, comparison of convergence properties with classical Neumann type expansions have been presented here.

We consider the generalized eigenvalue problem with the baseline deterministic system matrices as

$$\mathbf{K}_0\boldsymbol{\phi}_k = \lambda_k\mathbf{M}_0\boldsymbol{\phi}_k; \quad k = 1, 2, \ldots n \tag{15}$$

The eigenvalue and eigenvector matrix of the above system is denoted as $\lambda_0 = \text{diag}[\lambda_1, \lambda_2, \ldots, \lambda_n] \in \mathbb{R}^{n\times n}$ and $\boldsymbol{\Phi} = [\boldsymbol{\phi}_1, \boldsymbol{\phi}_2, \ldots, \boldsymbol{\phi}_n] \in \mathbb{R}^{n\times n}$. Here $\lambda_1 < \lambda_2 < \ldots < \lambda_n$ with orthonormal modal matrix $\boldsymbol{\Phi}$ which gives $\boldsymbol{\Phi}^T\mathbf{K}_0\boldsymbol{\Phi} = \lambda_0$ and $\boldsymbol{\Phi}^T\mathbf{M}_0\boldsymbol{\Phi} = \mathbf{I}$. Since the undamped eigenvectors $\boldsymbol{\phi}_k$ for $k = 1, 2, \ldots n$ form a complete basis, the solution of Eq. (12), $\tilde{\mathbf{u}}(\omega, \theta)$ can be projected to on this basis. Using the relations in Eqs. (13) and (15) we have

$$\boldsymbol{\Phi}^T\mathbf{A}_0\boldsymbol{\Phi} = \boldsymbol{\Phi}^T\big([-\omega^2 + i\omega\zeta_1]\mathbf{M}_0 + [i\omega\zeta_2 + 1]\mathbf{K}_0\big)\boldsymbol{\Phi}$$
$$= \big(-\omega^2 + i\omega\zeta_1\big)\mathbf{I} + \big(i\omega\zeta_2 + 1\big)\lambda_0 \tag{16}$$

We denote $\boldsymbol{\Phi}^T\mathbf{A}_0\boldsymbol{\Phi} = \boldsymbol{\Lambda}_0$ and $\mathbf{A}_0 = \boldsymbol{\Phi}^{-T}\boldsymbol{\Lambda}_0\boldsymbol{\Phi}^{-1}$ where $\boldsymbol{\Lambda}_0 = \big(-\omega^2 + i\omega\zeta_1\big)\mathbf{I} + \big(i\omega\zeta_2 + 1\big)\lambda_0$ and $\mathbf{I}$ is the identity matrix. We also introduce the transformations:

$$\widetilde{\mathbf{A}}_i = \boldsymbol{\Phi}^T\mathbf{A}_i\boldsymbol{\Phi} \quad \text{and} \quad \mathbf{A}_i$$
$$= \boldsymbol{\Phi}^{-T}\widetilde{\mathbf{A}}_i\boldsymbol{\Phi}^{-1} \text{ where } \widetilde{\mathbf{A}}_i, \in \mathbb{C}^{n\times n}; \quad \mathbf{A}_i \in \mathbb{C}^{n\times n}; \quad \forall\, i$$
$$= 1, 2, \ldots, M \tag{17}$$

Note that $\widetilde{\mathbf{A}}_0 = \boldsymbol{\Lambda}_0$ is a diagonal matrix. Substituting the expressions given in Eqs. (16) and (17) to Eq. (12) we can write

$$\tilde{\mathbf{u}}(\omega, \theta) = \left[\boldsymbol{\Phi}^{-T}\boldsymbol{\Lambda}_0(\omega)\boldsymbol{\Phi}^{-1} + \sum_{i=1}^{M} \xi_i(\theta)\boldsymbol{\Phi}^{-T}\widetilde{\mathbf{A}}_i(\omega)\boldsymbol{\Phi}^{-1}\right]^{-1}\tilde{\mathbf{f}}_0(\omega)$$
$$= \boldsymbol{\Phi}\boldsymbol{\Psi}(\omega, \boldsymbol{\xi}(\theta))\boldsymbol{\Phi}^T\tilde{\mathbf{f}}_0(\omega) \tag{18}$$

where $\boldsymbol{\Psi}(\omega, \boldsymbol{\xi}(\theta)) = [\boldsymbol{\Lambda}_0(\omega) + \sum_{i=1}^{M} \xi_i(\theta)\widetilde{\mathbf{A}}_i(\omega)]^{-1}$ and the M-dimensional random vector $\boldsymbol{\xi}(\theta)$ is given as $\boldsymbol{\xi}(\theta) = \{\xi_1(\theta), \xi_2(\theta), \ldots, \xi_M(\theta)\}^T$. The matrix $\widetilde{\mathbf{A}}_i$ can be written in terms of it's diagonal and off-diagonal terms as $\widetilde{\mathbf{A}}_i = \boldsymbol{\Lambda}_i + \boldsymbol{\Delta}_i$, $i = 1, 2, \ldots, M$. Here the diagonal matrix is $\boldsymbol{\Lambda}_i = \text{diag}[\widetilde{\mathbf{A}}_i] = \text{diag}[\Lambda_{i_1}, \Lambda_{i_2}, \ldots, \Lambda_{i_n}] \in \mathbb{C}^{n\times n}$ and the matrix containing only the off-diagonal elements $\boldsymbol{\Delta}_i = \widetilde{\mathbf{A}}_i - \boldsymbol{\Lambda}_i$ is such that $\text{Trace}(\boldsymbol{\Delta}_i) = 0$. Using these, from Eq. (18) one has

$$\boldsymbol{\Psi}(\omega, \boldsymbol{\xi}(\theta)) = \left[\underbrace{\boldsymbol{\Lambda}_0(\omega) + \sum_{i=1}^{M} \xi_i(\theta)\boldsymbol{\Lambda}_i(\omega)}_{\boldsymbol{\Lambda}(\omega,\boldsymbol{\xi}(\theta))} + \underbrace{\sum_{i=1}^{M} \xi_i(\theta)\boldsymbol{\Delta}_i(\omega)}_{\boldsymbol{\Delta}(\omega,\boldsymbol{\xi}(\theta))} \right]^{-1} \tag{19}$$

where $\boldsymbol{\Lambda}(\omega, \boldsymbol{\xi}(\theta)) \in \mathbb{C}^{n\times n}$ is a diagonal matrix and $\boldsymbol{\Delta}(\omega, \boldsymbol{\xi}(\theta))$ is an off-diagonal only matrix. Thus $\boldsymbol{\Psi}(\omega, \boldsymbol{\xi}(\theta)) = [\boldsymbol{\Lambda}(\omega, \boldsymbol{\xi}(\theta)) + \boldsymbol{\Delta}(\omega, \boldsymbol{\xi}(\theta))]^{-1}$.

We introduce the transformation of the stochastic system response to the modal coordinates such that $\widetilde{\mathbf{u}}(\omega, \theta) = \sum_i \Phi_i c_i(\omega, \theta) = [\boldsymbol{\Phi}]\{\mathbf{c}_i(\omega, \theta)\}$, where $\mathbf{c}(\omega, \theta) \in \mathbb{C}^n$ is the complex, frequency dependent modal response vector and following from Eqs. (18) and (19) we have

$$\begin{aligned} &\Big[\boldsymbol{\Lambda}(\omega, \boldsymbol{\xi}(\theta)) + \boldsymbol{\Delta}(\omega, \boldsymbol{\xi}(\theta))\Big]\mathbf{c}(\omega, \theta) = \boldsymbol{\Phi}^T\widetilde{\mathbf{f}}_0(\omega) \\ &\text{such that} \quad \mathbf{c}(\omega, \theta) = [\boldsymbol{\Lambda}(\omega, \boldsymbol{\xi}(\theta)) + \boldsymbol{\Delta}(\omega, \boldsymbol{\xi}(\theta))]^{-1}\boldsymbol{\Phi}^T\widetilde{\mathbf{f}}_0(\omega) \\ &= \boldsymbol{\Psi}\Big(\omega, \boldsymbol{\xi}(\theta)\Big)\boldsymbol{\Phi}^T\widetilde{\mathbf{f}}_0(\omega) \end{aligned} \tag{20}$$

The m-th order Neumann matrix series representation of $\mathbf{c}(\omega, \theta)$ in the above equation is given as

$$\mathbf{c}(\omega, \theta) = \boldsymbol{\Psi}^{(m)}\Big(\omega, \boldsymbol{\xi}(\theta)\Big)\boldsymbol{\Phi}^T\widetilde{\mathbf{f}}_0(\omega) = \boldsymbol{\Gamma}^{(m)}\Big(\omega, \boldsymbol{\xi}(\theta)\Big) \tag{21}$$

$$\begin{aligned} &\text{where} \quad \boldsymbol{\Psi}^{(m)}(\omega, \boldsymbol{\xi}(\theta)) \\ &= \sum_{s=0}^{m-1} (-1)^s[\boldsymbol{\Lambda}^{-1}(\omega, \boldsymbol{\xi}(\theta))\boldsymbol{\Delta}(\boldsymbol{\xi}(\theta))]^s\boldsymbol{\Lambda}^{-1}(\omega, \boldsymbol{\xi}(\theta)) \end{aligned} \tag{22}$$

where $\boldsymbol{\Gamma}^{(m)}(\omega, \boldsymbol{\xi}(\theta)) = \{\Gamma_1^{(m)}(\omega, \boldsymbol{\xi}(\theta)), \ldots, \Gamma_n^{(m)}(\omega, \boldsymbol{\xi}(\theta))\}^T$ is the vector of complex frequency dependent stochastic coefficients. The stochastic response vector is thus given as

$$\widetilde{\mathbf{u}}^{(m)}(\omega, \theta) = \sum_{k=1}^{n} \Gamma_k^{(m)}(\omega, \boldsymbol{\xi}(\theta))\boldsymbol{\phi}_k \tag{23}$$

The solution vector $\widetilde{\mathbf{u}}(\theta)$ is projected in the space spanned by $\boldsymbol{\phi}_k$ and weighted by $\Gamma_k^{(m)}(\omega, \boldsymbol{\xi}(\theta))$ which are referred to as m-th order 'spectral functions' [20]. Computational efficiency demands that a good solution approximation is obtained even when using a moderate value of m. It can be seen from Eq. (23) that the stochastic system response is given by a linear combination of fundamental vibration modes $\boldsymbol{\phi}_k$ weighted by the stochastic spectral functions Γ_k.

3.3. Properties of the frequency-dependent spectral functions

A closer look at these spectral functions (from Eq. (22)) indicates that $\boldsymbol{\Lambda}^{-1}(\omega, \boldsymbol{\xi}(\theta))$ is a diagonal matrix with stochastic elements while $\boldsymbol{\Delta}(\omega, \boldsymbol{\xi}(\theta))$ is a stochastic off-diagonal only matrix. This results in the spectral functions to be a *rational functions* of the basic random variables. In contrast the classical Neumann expansion technique or the polynomial chaos based methods expands the stochastic solution using series of polynomials of the basic random variables. The convergence of the series in Eq. (22) depends of the spectral radius of $\mathbf{R}(\omega, \boldsymbol{\xi}(\theta)) = \boldsymbol{\Lambda}^{-1}(\omega, \boldsymbol{\xi}(\theta))\boldsymbol{\Delta}(\omega, \boldsymbol{\xi}(\theta))$ a generic term of which is given as

$$R_{rs} = \frac{\Delta_{rs}}{\Lambda_{rr}} = \frac{\sum_{i=1}^{M} \xi_i\Delta_{i_{rs}}}{\Lambda_{0_r} + \sum_{i=1}^{M} \xi_i\Lambda_{i_r}} = \frac{\sum_{i=1}^{M} \xi_i\widetilde{A}_{i_{rs}}}{\Lambda_{0_r} + \sum_{i=1}^{M} \xi_i\widetilde{A}_{i_{rr}}}; \; r \neq s \tag{24}$$

This indicates that the spectral radius of $\mathbf{R}(\omega, \boldsymbol{\xi}(\theta))$ is controlled by the diagonal dominance of the $\widetilde{\mathbf{A}}_i$ matrices. Especially near the resonance frequencies, where the radius of convergence of the system in classical Neumann expansion becomes quite small, the latter fails to converge. As a result the diagonal parts of the perturbation matrices have a significant role to play in the proposed methodology (demonstrated later in Fig. 11). Also since the spectral functions are frequency dependent, it ensures that their spectral radius is frequency adaptive in nature which is a significant advantage compared to the classical Neumann expansion technique.

A one term approximation of the series comprising the n elements of $\boldsymbol{\Gamma}^{(m)}(\omega, \boldsymbol{\xi}(\theta))$ in Eq. (23) such that $m=1$ is termed as the first-order spectral functions. This gives from Eq. (22) the first-order spectral functions as

$$\Gamma_k^{(1)}(\omega, \boldsymbol{\xi}(\theta)) = \frac{\boldsymbol{\phi}_k^T\widetilde{\mathbf{f}}_0(\omega)}{\Lambda_{0_k}(\omega) + \sum_{i=1}^{M} \xi_i(\theta)\Lambda_{i_k}(\omega)}; \quad k = 1, \ldots, n \tag{25}$$

Thus, $\Gamma_k^{(1)}(\omega, \boldsymbol{\xi}(\theta))$ are correlated and non-Gaussian random variables, which are rational function of the iid random variables $\xi_i(\theta)$. The response vector in terms of these spectral functions can be simplified to

$$\widetilde{\mathbf{u}}^{(1)}(\omega, \theta) = \sum_{k=1}^{n} \underbrace{\left(\frac{1}{\Lambda_k}\left[\boldsymbol{\phi}_k^T\widetilde{\mathbf{f}}_0(\omega)\right]\right)}_{\Gamma_k^{(1)}(\omega,\boldsymbol{\xi}(\theta))}\boldsymbol{\phi}_k \tag{26}$$

The above equation shows that the response vector approximated with first order spectral functions does not involve the 'interaction' between the different eigenmodes. The modal coefficients (spectral functions in this case) are stochastic in nature. This is different from the classical Neumann expansion scheme in that, for this same order of expansion, the system response for the latter case is exactly equal to the deterministic case and hence fails to capture any effect of parametric uncertainty. It would be seen in subsequent discussions that the system response when captured with these first order spectral functions only and facilitated by the Galerkin method produces results which are agreeable with the direct MCS simulation.

A two term approximation of the series in Eq. (22) gives the second-order spectral functions $\Gamma_k^{(2)}(\omega, \boldsymbol{\xi}(\theta))$ for $k=1,\ldots,n$ in terms of $\boldsymbol{\Psi}^{(2)}(\omega, \boldsymbol{\xi}(\theta)) = \boldsymbol{\Lambda}^{-1}(\omega, \boldsymbol{\xi}(\theta)) - \boldsymbol{\Lambda}^{-1}(\omega, \boldsymbol{\xi}(\theta))\boldsymbol{\Delta}(\omega, \boldsymbol{\xi}(\theta))\boldsymbol{\Lambda}^{-1}(\omega, \boldsymbol{\xi}(\theta))$. A generic element of $\boldsymbol{\Psi}^{(2)}(\omega, \boldsymbol{\xi}(\theta))$ is given as

$$\begin{aligned} \Psi_{kj}^{(2)}(\omega, \boldsymbol{\xi}(\theta)) &= \frac{\delta_{kj}}{\Lambda_{0_k}(\omega) + \sum_{i=1}^{M} \xi_i(\theta)\Lambda_{i_k}(\omega)} \\ &\quad - \frac{\sum_{i=1}^{M} \xi_i(\theta)\Delta_{i_{kj}}(\omega)}{\Big(\Lambda_{0_k}(\omega) + \sum_{i=1}^{M} \xi_i(\theta)\Lambda_{i_k}(\omega)\Big)\Big(\Lambda_{0_j}(\omega) + \sum_{i=1}^{M} \xi_i(\theta)\Lambda_{i_j}(\omega)\Big)} \end{aligned}$$

Hence the second-order spectral functions can be written in explicitly as

$$\begin{aligned} \Gamma_k^{(2)}(\omega, \boldsymbol{\xi}(\theta)) &= \frac{\boldsymbol{\phi}_k^T\widetilde{\mathbf{f}}_0(\omega)}{\Lambda_{0_k}(\omega) + \sum_{i=1}^{M} \xi_i(\theta)\Lambda_{i_k}(\omega)} \\ &\quad - \sum_{\substack{j=1 \\ j\neq k}}^{n} \frac{(\boldsymbol{\phi}_j^T\widetilde{\mathbf{f}}_0(\omega)) \sum_{i=1}^{M} \xi_i(\theta)\Delta_{i_{kj}}(\omega)}{\Big(\Lambda_{0_k}(\omega) + \sum_{i=1}^{M} \xi_i(\theta)\Lambda_{i_k}(\omega)\Big)\Big(\Lambda_{0_j}(\omega) + \sum_{i=1}^{M} \xi_i(\theta)\Lambda_{i_j}(\omega)\Big)} \end{aligned}$$

The second-order terms can be viewed as adding the modal coupling in the approximation of the system response when compared to Eq. (25). The stochastic response vector can thus be written as

$$\tilde{\mathbf{u}}^{(2)}(\omega,\theta)=\tilde{\mathbf{u}}^{(1)}(\omega,\theta)-\sum_i\left(\sum_j(1-\delta_{ij})Q_{ij}(\boldsymbol{\phi}_j^T\tilde{\mathbf{f}}_0(\omega))\right)\boldsymbol{\phi}_i \tag{27}$$

where Q_{ij} is are the elements of the matrix $\mathbf{Q}=\boldsymbol{\Lambda}^{-1}\left(\omega,\boldsymbol{\xi}(\theta)\right)\boldsymbol{\Delta}\left(\omega,\boldsymbol{\xi}(\theta)\right)\boldsymbol{\Lambda}^{-1}\left(\omega,\boldsymbol{\xi}(\theta)\right)$ which is the second term in the expression for $\Gamma_k^{(2)}\left(\omega,\boldsymbol{\xi}(\theta)\right)$. The matrix $\mathbf{Q}$ is an off-diagonal only matrix and $(1-\delta_{ij})$ has been introduced to indicate this clearly. Hence from Eq. (27) it is clear that the introduction of the second order terms helps to take into account the stochastic coupling of the eigen modes of the system.

The vector of spectral functions of order m can be obtained by retaining m terms in the series Eq. (22) and can be expressed as

$$\boldsymbol{\Gamma}^{(m)}(\omega,\boldsymbol{\xi}(\theta))=\left[\mathbf{I}_n-\mathbf{R}(\omega,\boldsymbol{\xi}(\theta))+\mathbf{R}(\omega,\boldsymbol{\xi}(\theta))^2-\mathbf{R}(\omega,\boldsymbol{\xi}(\theta))^3\ldots m^{\text{th}}\text{ term}\right]\boldsymbol{\Gamma}^{(1)}(\omega,\boldsymbol{\xi}(\theta)) \tag{28}$$

where $\mathbf{I}_n$ is the n-dimensional identity matrix with $\mathbf{R}$ defined in Eq. (24). It can be noted that in general

$$\tilde{\mathbf{u}}^{(m)}(\omega,\theta)=\tilde{\mathbf{u}}^{(m-1)}(\omega,\theta)+(-1)^{m-1}\sum_i\left(\sum_j Q_{ij}^{(m)}(\boldsymbol{\phi}_j^T\tilde{\mathbf{f}}_0(\omega))\right)\boldsymbol{\phi}_i\quad\forall\, m>2 \tag{29}$$

where $Q_{ij}^{(m)}$ are the elements of the matrix $\mathbf{Q}^{(m)}=(\boldsymbol{\Lambda}^{-1}(\omega,\boldsymbol{\xi}(\theta))\boldsymbol{\Delta}(\omega,\boldsymbol{\xi}(\theta)))^{m-1}\boldsymbol{\Lambda}^{-1}(\omega,\boldsymbol{\xi}(\theta))$. The matrix $\mathbf{Q}^{(m)}$ is a full rank matrix and denotes the coupling of the eigen modes of the deterministic system to represent the solution of the stochastic system.

The essential features of the proposed approach for the resolution of the frequency domain response of randomly parameterized systems can be summarized as follows:

- The frequency domain response of the randomly parameterized vibrating system has been expressed with non-linear, frequency adaptive, rational functions of the basic random variables, called spectral functions.
- The stochastic system response is expressed with a set of eigenmodes of the model weighted by the spectral functions.
- The convergence radius of these spectral functions is frequency adaptive which ensures good convergence of the solution even near the resonance frequencies of the system.
- The expression for the low-order spectral functions have been obtained explicitly in terms of the stochastic parameters which highlights the stochastic coupling of the eigenmodes of the system.

The above points distinguish the proposed approach from the existing Galerkin projection schemes in terms of novelty and computational efficiency. It must be highlighted though that when using higher order spectral functions to approximate the stochastic response system, the additional computational cost can be offset by using a Bayesian metamodel [21]. In the following section we discuss the aspect of frequency dependence of the spectral functions.

3.4. Frequency dependence of the spectral functions

From Eq. (23), it can be observed that the spectral functions are not general basis functions, but are *specific* to the stochastic system being solved. The frequency content, as well as the forcing function, has a significant influence on the behavior of the spectral functions. Here we consider the applied force to be uniform in the frequency domain which helps in understanding the general nature of the frequency dependence of the spectral functions clearly.

Fig. 1 shows the plot of the absolute values of the first seven complex spectral functions obtained for a particular random sample and for different values of standard deviation σ_a of the underlying random field.

These spectral functions have been calculated for the bending vibration of the Euler-Bernoulli cantilever beam presented later in Section 6.1. A unit harmonic force applied at the free end of the cantilever beam is considered. The frequency response of each spectral function shows that their peaks correspond to the frequencies of the fundamental eigen modes with which they are associated. Also it is observed that for higher values of σ_a, the modal coupling increases, as is demonstrated by an increase in the spectral function amplitudes at other modal frequencies than those with which they are associated individually. This can be explained as follows: an increases in the variability of the random field results in a greater contribution of the deviatoric parts of the system matrices in Eq. (12). This modification of the system matrices would be reflected in an enhanced interaction between the structural modes of the beam which can be seen from Eq. (22).

Fig. 2 shows the different orders (2, 3 and 4) of the spectral function associated with the eigen modes i.e. $\Gamma_k^{(m)}(\omega,\boldsymbol{\xi}(\theta_j))$ for $m=2,3,4$; $k=2,3,\ldots,7$ and θ_j being a sample realization in the probability space.

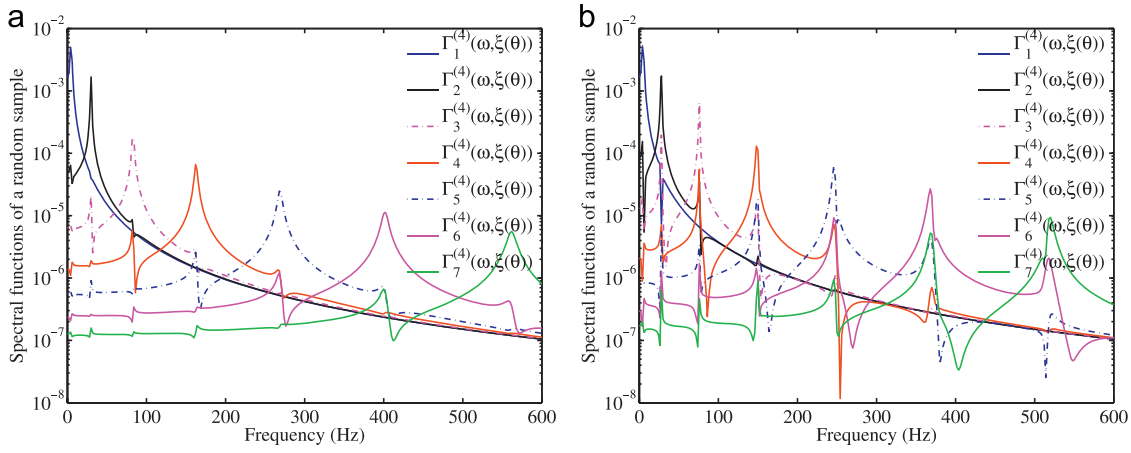

Fig. 1. The amplitude of the first seven spectral functions of order 4 for a particular random sample under applied force. The spectral functions are obtained for two different standard deviation levels of the underlying random field: $\sigma_a=\{0.05, 0.20\}$. (a) Spectral functions for $\sigma_a=0.05$. (b) Spectral functions for $\sigma_a=0.2$.

It shows the effect of the sample modal contributions expressed in terms of the stochastic spectral functions. Increasing the order of the spectral functions would give a better solution approximation, especially near the resonance frequencies, but involves added computational cost. Thus the model reduction has to be performed judiciously which is discussed in the following section.

4. Model reduction and Galerkin error minimization technique

4.1. Modal truncation

The classical approach on reducing the number of modal basis used for the construction of the approximate solution is guided by the cut-off frequency (Nyquist frequency), wherein the higher mode shapes are considered unimportant and done away with. Thus the system response is formulated with the n_r truncated modal basis so that

$$\frac{\omega}{\omega_j} << 1, \quad \text{for } j > n_r \tag{30}$$

where ω_j is the natural frequency of the jth mode and $\omega \in \Omega$ is the frequency domain. Thus, $n_r \leq n$ results in lower computational cost for resolving the system equations.

For the stochastic system, parametric uncertainty results in the distribution of the stochastic natural frequencies around those of the baseline model. The spectral functions weighting the eigen basis are stochastic in nature and hence the contribution of the various modes may vary with the sample number. Using the first order spectral function $\Gamma_k^{(1)}(\omega, \boldsymbol{\xi}(\theta)) = (\boldsymbol{\phi}_k^T \tilde{\mathbf{f}}_0(\omega))/(\Lambda_{0_k}(\omega) + \sum_{i=1}^{M} \xi_i(\theta)\Lambda_{i_k}(\omega))$, it is observed that the stochastic weighting coefficients modify the contributions of the individual vibration modes based on the nature of the element perturbation matrices $\Lambda_{i_k}(\omega)$. For higher values of standard deviation, the effect becomes more significant. Hence, it is suggested to go beyond the Nyquist criterion and include a greater number of modal bases in approximating the stochastic system solution.

Following from Eq. (23), the approximate solution can be represented with a reduced number (n_r) of modal basis as

$$\tilde{\mathbf{u}}(\omega, \theta) \approx \sum_{k=1}^{n_r} \hat{\Gamma}_k^{(m)}(\omega, \boldsymbol{\xi}(\theta))\boldsymbol{\phi}_k \tag{31}$$

where $\hat{\Gamma}_k^{(m)}(\omega, \boldsymbol{\xi}(\theta))$ are m-th order stochastic spectral functions and $\boldsymbol{\phi}_k$ are the eigen vectors of the deterministic system respectively. The accuracy of this series in Eq. (31) can be improved in two ways: (a) by increasing the number of modal basis (n_r) or (b) by increasing the order m of the spectral functions $\hat{\Gamma}_k^{(m)}(\boldsymbol{\xi}(\omega, \theta))$. This study has made use of the eigen modes that are within three to four times the frequency range of interest of the problem at hand. It should be noted, though, that the truncation of the series given in Eq. (31) introduces approximation errors into the solution vector which has been analyzed for the examples considered in this paper.

4.2. Galerkin type error minimization

It has been shown from the discussion in previous sections that various orders of spectral functions obtained by truncating an infinite series expansion as well as using the well-established model reduction techniques help alleviate much of the computational burden by reducing the dimensionality of the stochastic system. However, the error introduced due to the finite order approximation of the spectral functions and the use of a reduced number of modal basis induces solution errors. The idea here is to introduce a Galerkin-type orthogonalization of the residual to the modal basis functions with the aim of reducing this truncation error. We express the solution vector by the series representation:

$$\tilde{\mathbf{u}}(\omega, \theta) = \sum_{k=1}^{n_r} c_k(\omega)\hat{\Gamma}_k(\omega, \boldsymbol{\xi}(\theta))\boldsymbol{\phi}_k \tag{32}$$

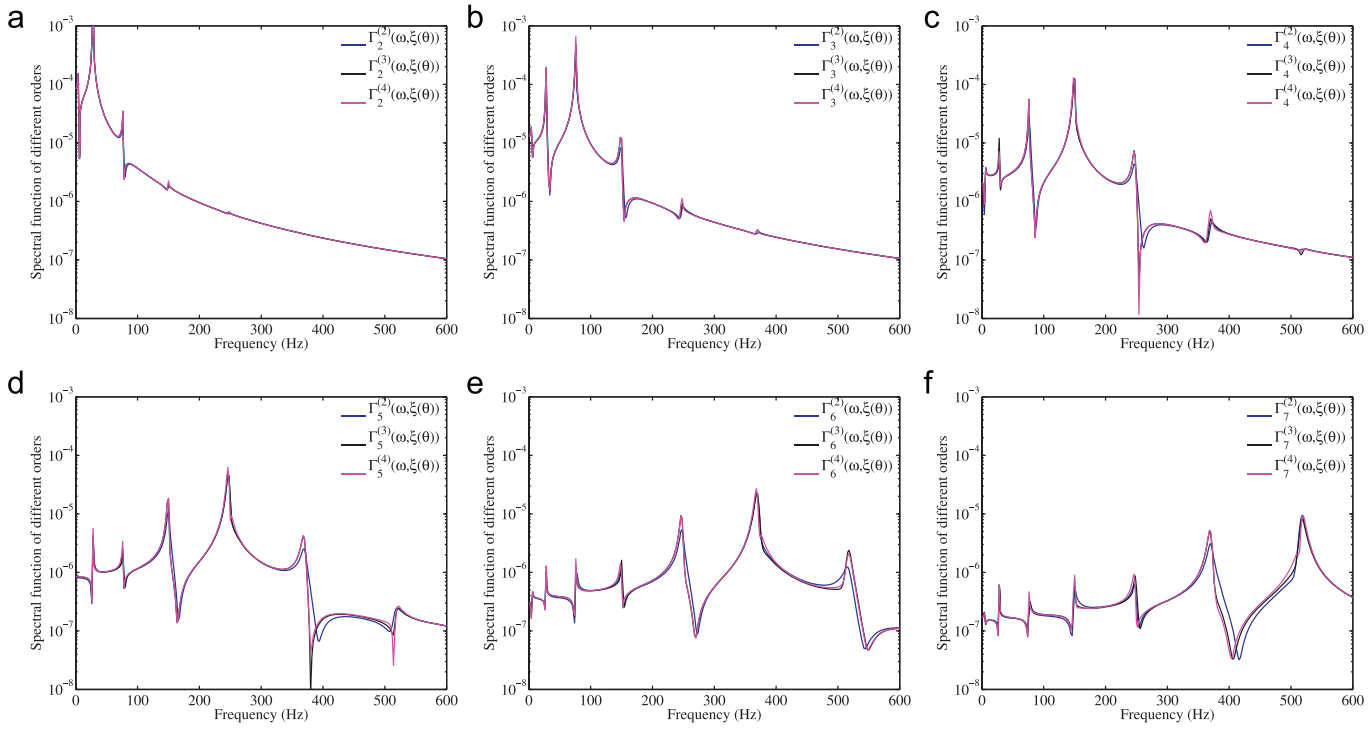

Fig. 2. The frequency domain response of the spectral functions, $\Gamma_k^{(m)}(\omega, \boldsymbol{\xi}(\theta))$ of orders $m = 2, 3, 4$. The spectral functions are obtained for a particular random sample and for $\sigma_a = 0.20$. (a) Different orders of $\Gamma_2(\omega, \boldsymbol{\xi}(\theta))$. (b) Different orders of $\Gamma_3(\omega, \boldsymbol{\xi}(\theta))$. (c) Different orders of $\Gamma_4(\omega, \boldsymbol{\xi}(\theta))$. (d) Different orders of $\Gamma_5(\omega, \boldsymbol{\xi}(\theta))$. (e) Different orders of $\Gamma_6(\omega, \boldsymbol{\xi}(\theta))$. (f) Different orders of $\Gamma_7(\omega, \boldsymbol{\xi}(\theta))$.

where the functions $\widehat{\Gamma}_k$ are the spectral functions of finite order (as given in Eq. (31)), $\boldsymbol{\phi}_k \in \mathbb{R}^n$ are the eigenvectors introduced earlier in Eq. (15) and the constants $c_k(\omega) \in \mathbb{C}$ for a given value of the frequency has to be obtained using the Galerkin approach. Substituting the expansion of $\widetilde{\mathbf{u}}(\omega, \theta)$ in the governing equation (12), the residual vector is given by

$$\boldsymbol{\varepsilon}(\omega, \theta) = \left(\sum_{i=0}^{M} \mathbf{A}_i(\omega)\xi_i(\theta)\right)\left(\sum_{k=1}^{n_r} c_k(\omega)\widehat{\Gamma}_k(\omega, \boldsymbol{\xi}(\theta))\boldsymbol{\phi}_k\right) - \tilde{\mathbf{f}}_0(\omega) \in \mathbb{C}^n \tag{33}$$

where $\xi_0 = 1$ is used to simplify the first summation expression. The expression in Eq. (32) can be viewed as a projection of the solution vector on to the deterministic modal basis weighed by the complex frequency dependent stochastic weighting functions $\widehat{\Gamma}_k(\omega, \boldsymbol{\xi}(\theta))$. Thus we wish to obtain the coefficients $c_k(\omega)$ using the Galerkin approach so that the residual is made orthogonal to the eigen basis in the mean sense at each frequency step, i.e. mathematically

$$\langle \boldsymbol{\phi}_j, \boldsymbol{\varepsilon}(\omega, \theta)\rangle = 0 \quad \forall\, j = 1, 2, \ldots, n_r \tag{34}$$

Here $\langle \mathbf{u}(\theta), \mathbf{v}(\theta)\rangle = \int_\Theta \mathbf{u}(\theta)\mathbf{v}(\theta)P(\mathrm{d}\theta)$ defines the inner product norm. Imposing this condition and using the expression of $\boldsymbol{\varepsilon}(\omega, \theta)$ from Eq. (33) one has

$$\mathbb{E}\left[\boldsymbol{\phi}_j^T\left(\sum_{i=0}^{M} \mathbf{A}_i(\omega)\xi_i(\theta)\right)\left(\sum_{k=1}^{n_r} c_k(\omega)\widehat{\Gamma}_k(\omega, \boldsymbol{\xi}(\theta))\boldsymbol{\phi}_k\right) - \boldsymbol{\phi}_j^T\tilde{\mathbf{f}}_0(\omega)\right] = 0 \tag{35}$$

Interchanging the $\mathbb{E}[\bullet]$ and summation operations, this can be simplified to

$$\sum_{k=1}^{n_r}\left(\sum_{i=0}^{M} \underbrace{\left(\boldsymbol{\phi}_j^T\mathbf{A}_i(\omega)\boldsymbol{\phi}_k\right)}_{\widetilde{A}_{ijk}(\omega)}\underbrace{\mathbb{E}\left[\xi_i(\omega, \theta)\widehat{\Gamma}_k(\omega, \boldsymbol{\xi}(\theta))\right]}_{D_{ik}(\omega)}\right)c_k(\omega) = (\boldsymbol{\phi}_j^T\tilde{\mathbf{f}}_0(\omega)) \tag{36}$$

Defining the vector $\mathbf{c}(\omega) = \{c_1(\omega), c_2(\omega), \ldots, c_n(\omega)\}^T$, these equations can be expressed as

$$\mathbf{S}(\omega)\mathbf{c}(\omega) = \mathbf{b}(\omega) \tag{37}$$

with $S_{jk}(\omega) = \sum_{i=0}^{M}\widetilde{A}_{i_{jk}}(\omega)D_{ik}(\omega)$; $\forall\, j, k = 1, 2, \ldots, n_r$ where the expressions $\widetilde{A}_{i_{jk}}(\omega) = \boldsymbol{\phi}_j^T\mathbf{A}_i(\omega)\boldsymbol{\phi}_k$, $D_{ik}(\omega) = \mathbb{E}\left[\xi_i(\theta)\widehat{\Gamma}_k(\omega, \boldsymbol{\xi}(\theta))\right]$ and $b_j(\omega) = \left(\boldsymbol{\phi}_j^T\tilde{\mathbf{f}}_0(\omega)\right)$. The number of equations to be solved for the unknown coefficients in Eq. (37) is n_r which is the dimension of the reduced system in the modal coordinates represented by Eq. (32).

5. Calculation of the dynamic response statistics

For practical application of the method developed here, the efficient computation of the response moments and pdf is important. A simulation based algorithm is proposed in this section. The coefficient vector $\mathbf{c} \in \mathbb{C}^{n_r}$ in Eq. (32) can be calculated from a reduced set of equations given by Eq. (37). Once these coefficients are calculated, the statistical moments of the solution can be obtained from Eqs. (38) and (39) using the Monte Carlo simulation. The spectral functions used to obtain the vector $\mathbf{c}$ itself can to be reused to obtain the statistics and pdf of the solution. The mean vector can be obtained as

$$\bar{\mathbf{u}}(\omega) = \mathbb{E}\left[|\widetilde{\mathbf{u}}(\omega, \theta)|\right] = \sum_{k=1}^{n_r}|c_k|\mathbb{E}\left[\left|\widehat{\Gamma}_k(\omega, \boldsymbol{\xi}(\theta))\right|\right]\boldsymbol{\phi}_k \tag{38}$$

where $|\bullet|$ is the absolute value of the complex quantities. The covariance matrix of the solution vector is

$$\begin{aligned}\boldsymbol{\Sigma}_u(\omega) &= \mathbb{E}\left[\left(|\widetilde{\mathbf{u}}(\omega, \theta)| - \bar{\mathbf{u}}(\omega)\right)\left(|\widetilde{\mathbf{u}}(\omega, \theta)| - \bar{\mathbf{u}}(\omega)\right)^T\right] \\ &= \sum_{k=1}^{n_r}\sum_{j=1}^{n_r}\left|c_kc_j\right|\Sigma_{\Gamma_{kj}}(\omega)\boldsymbol{\phi}_k\boldsymbol{\phi}_j^T\end{aligned} \tag{39}$$

where the elements of the covariance matrix of the spectral functions are given by

$$\begin{aligned}\Sigma_{\Gamma_{kj}}(\omega) = \mathbb{E}\Big[&\left(\left|\widehat{\Gamma}_k(\omega, \boldsymbol{\xi}(\theta))\right| - \mathbb{E}\left[\left|\widehat{\Gamma}_k(\omega, \boldsymbol{\xi}(\theta))\right|\right]\right) \\ &\left(\left|\widehat{\Gamma}_j(\omega, \boldsymbol{\xi}(\theta))\right| - \mathbb{E}\left[\left|\widehat{\Gamma}_j(\omega, \boldsymbol{\xi}(\theta))\right|\right]\right)\Big]\end{aligned} \tag{40}$$

Considering the fact that the elements of the vector $\widetilde{\mathbf{u}}(\omega, \theta)$ are complex valued non-stationary random processes, further statistical properties can also be obtained. For example one can calculate the two-point auto-correlation function of the absolute value as

$$\begin{aligned}\boldsymbol{\Sigma}_u(\omega_1, \omega_2) &= \mathbb{E}\left[\left(|\widetilde{\mathbf{u}}(\omega_1, \theta)| - \bar{\mathbf{u}}(\omega_1)\right)\left(|\widetilde{\mathbf{u}}(\omega_2, \theta)| - \bar{\mathbf{u}}(\omega_2)\right)^T\right] \\ &= \sum_{k=1}^{n_r}\sum_{j=1}^{n_r}\left|c_kc_j\right|\Sigma_{\Gamma_{kj}}(\omega_1, \omega_2)\boldsymbol{\phi}_k\boldsymbol{\phi}_j^T\end{aligned} \tag{41}$$

where the elements of the covariance matrix of the spectral functions are given by

$$\begin{aligned}&\Sigma_{\Gamma_{kj}}(\omega_1, \omega_2) \\ &= \mathbb{E}\Big[\left(\left|\widehat{\Gamma}_k(\omega_1, \boldsymbol{\xi}(\theta))\right| - \mathbb{E}\left[\left|\widehat{\Gamma}_k(\omega_1, \boldsymbol{\xi}(\theta))\right|\right]\right) \\ &\quad\left(\left|\widehat{\Gamma}_j(\omega_2, \boldsymbol{\xi}(\theta))\right| - \mathbb{E}\left[\left|\widehat{\Gamma}_j(\omega_2, \boldsymbol{\xi}(\theta))\right|\right]\right)\Big]\end{aligned} \tag{42}$$

Based on the results derived in the paper, a hybrid reduced simulation-analytical approach can thus be realized in practice. The method is applicable to general structural dynamics problems with general non-Gaussian random fields. In the following section this approach has been applied to two physical problems.

6. Illustrative application: The stochastic analysis of an Euler–Bernoulli beam and a Kirchhoff–Love plate

We present some numerical studies with classical structural dynamic systems to demonstrate the effectiveness of the proposed spectral function approach. The solution is obtained for a random field model of the input parametric uncertainty for various degrees of input variability. Direct MCS solution has been performed for these cases and is taken as the benchmark solution with respect to which the accuracy of the proposed methods have been analyzed. A comparison between the Polynomial Chaos expansion, Neumann expansion and the proposed approach has also been presented.

6.1. Case I: Euler–Bernoulli beam

In this section we apply the computational method to a cantilever beam clamped at one end (where the displacement and the rotational degree of freedom is set to zero). Fig. 3(a) shows the configuration of the cantilever beam with a harmonic point load at its free end. We assume that the bending modulus (EI) is a stationary Gaussian random field of the form:

$$EI(x, \theta) = EI_0(1 + a(x, \theta)) \tag{43}$$

where x is the coordinate along the length of the beam, EI_0 is the mean bending modulus, $a(x, \theta)$ is a zero mean stationary Gaussian random field.

The covariance kernel of this random field is taken to be of the form:

$$C_a(x_1, x_2) = \sigma_a^2 e^{-(|x_1 - x_2|)/\mu_a} \tag{44}$$

where μ_a is the correlation length and σ_a is the standard deviation. The base-line parameters are chosen as $L = 1$ m, cross-section $(b \times h)39 \times 5.93\ \text{mm}^2$ and Young's modulus $E = 2 \times 10^{11}$ Pa. In study we consider deflection of the tip of the beam under harmonic loads of amplitude $\tilde{f}_0 = 1.0N$. The correlation length considered in this numerical study is $\mu_a = L/2$. The number of terms used to represent the discretized random field in the spatial domain is chosen as $M = 2$. For the finite element discretization, the beam is divided into 100 elements. Standard four degrees of freedom Euler–Bernoulli beam model is used. After applying the fixed boundary condition at one edge, we obtain the number of degrees of freedom of the model to be $n = 200$. It has been verified that this spatial resolution is sufficient for the frequency of excitation considered in this study.

The dynamic analysis of the cantilever beam has been done for the case of unit amplitude harmonic point load acting on the free end of the beam over a frequency range of 0–600 Hz at an interval of 2 Hz. The solution of the proposed reduced basis spectral method has been compared with the direct MCS results and the 4th order PC expansion. The simulations have been performed with 10,000 MCS samples and for four different values of σ_a, which is the standard deviation of the random bending stiffness of the beam, with the aim of simulating different levels of uncertainty.

Fig. 3(b) presents the distribution of the natural frequencies of the cantilever beam, which are the square root of the eigenvalues λ_k of the generalized eigenvalues (Eq. (15)) of the dynamic beam problem. The reduced basis of the problem should be chosen

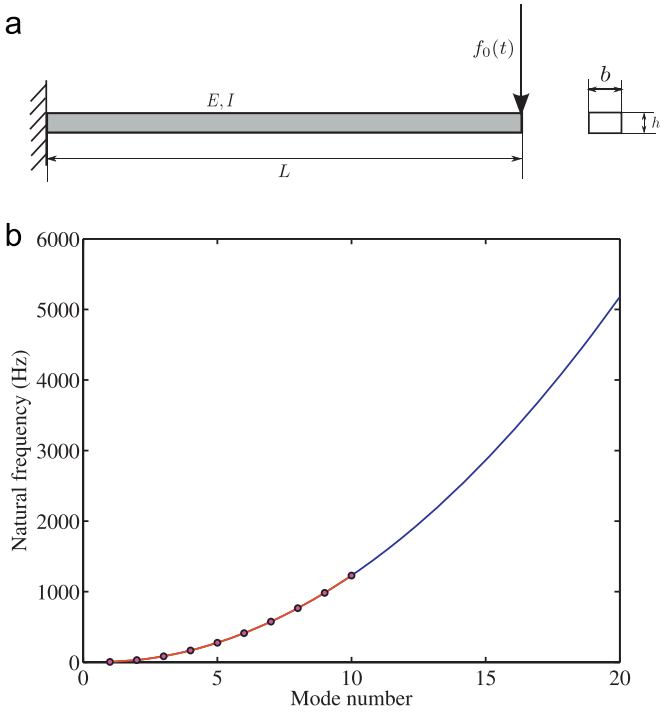

Fig. 3. Schematic diagram of the cantilever beam with a harmonic point load at the free end along with its natural frequencies. The number of reduced eigenvectors chosen is $q = 10$ which covers upto twice (1200 Hz) the frequency range of interest (600 Hz). (a) Schematic diagram of the beam with a point load at the free end. (b) Natural frequency of the cantilever beam.

based on the frequency range of interest of this particular problem, i.e. all the eigen modes that covers up to 1200 Hz must be included in the formulation (given that the maximum frequency in the study is 600 Hz). However, based on the discussion given in Section 4.1, 10 eigen modes have been selected. We have applied a constant modal damping matrix with 1% damping factor for all the modes. Here the mass and damping matrices are assumed to be deterministic in nature. However, the proposed theoretical approach is general and equally applicable for random mass, stiffness and damping matrices.

The frequency response of the mean deflection of the tip of the beam is shown in Fig. 4 for two values of σ_a and for unit amplitude harmonic point load at the free end. The figures show a comparison of the reduced basis spectral method results with the direct MCS simulation and the 4th order polynomial chaos solution. A plot of the deterministic system response is also included for reference. The spectral solution has been obtained for different orders of the solution following Eq. (22), where the orders $s = 2, 3, 4$. Since we consider the first 10 eigenmodes of the solution, the Galerkin method necessitates the solution of a 10×10 linear system of equations to obtain the undetermined coefficients associated with the response, as given in Eq. (37). In contrast, for the PC solution technique using 4th order polynomial functions, it is essential to solve a 3000×3000 dimensional linear system of equations in order to obtain the undetermined coefficients associated with the Hermite polynomials at every frequency step.

A good agreement between the MCS simulation and the proposed spectral approach can be observed in Fig. 4. When compared with the deterministic system response, it shows that the uncertainty has an effect similar to that of damping at the resonance peaks. This can be explained by the fact that the parametric variation of the beam, results in its peak response for the different samples to get distributed around the resonance frequency zones instead of being concentrated at a particular frequency. As a results, when the subsequent averaging is applied, it smooths out the resonance peaks. The same explanation holds for the anti-resonance frequencies. It should however be pointed out that this is not a phenomenon of physical damping and there might still be a high amplitude deflection obtained for a particular random sample in practical problems. The 4th order PC solution shows an accurate mean response estimation at low frequencies for small variability (like for $\sigma_a = 0.05$) of the random field. However, the response becomes inconsistent for higher value of variability, especially at the resonance frequencies. This can lead to serious practical problem as the response near the resonance frequency is often the most crucial quantity of engineering interest.

As the response of the system is in terms of the spectral functions, it is now useful to understand the stochastic system response in terms of the statistical properties of the spectral functions. We show the plot of the first seven 4th order mean spectral functions $E[\widehat{\Gamma}_k(\omega, \boldsymbol{\xi}(\theta))]$ in Fig. 5 as function of frequency for two different values of variability of the random field. It is found that the resonance peak of each spectral function is obtained at the natural frequencies of the vibration modes with which they are associated and denotes mean of the stochastic modal amplitudes of the beam. Also, the amplitude of the functions at the resonance peaks is found to decrease for higher values of σ_a which is consistent with the observation in Fig. 4 that the effect of increased variability of the random field results in a damping type effect on the mean response. The ratio of the amplitudes of consecutive spectral functions at a resonance frequency increases with an increase in the value of σ_a. For e.g. the ratio of $E[\Gamma_6^4(\omega, \boldsymbol{\xi}(\theta))]/E[\Gamma_5^4(\omega, \boldsymbol{\xi}(\theta))]$ around 400 Hz is found to decrease with σ_a. This shows that the coupling of the vibration modes tend to increase with the increasing variability of the random field as

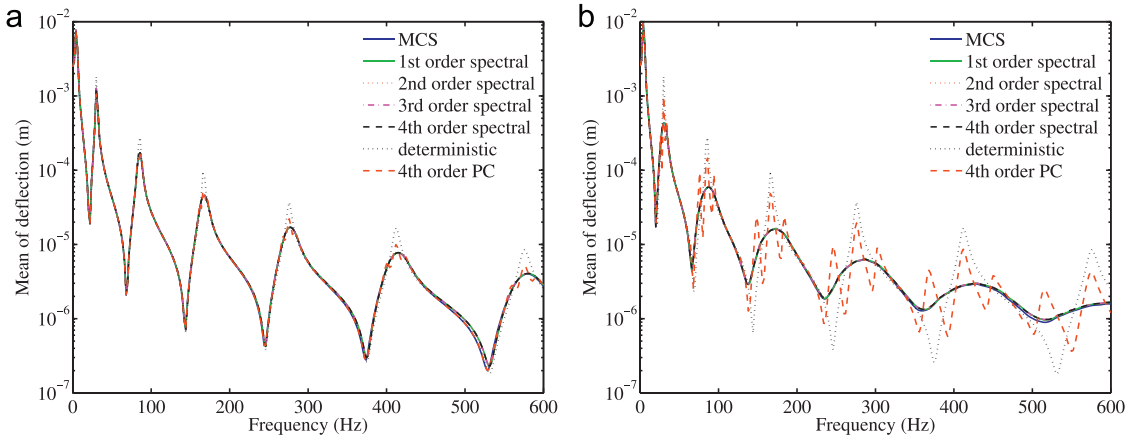

Fig. 4. The mean deflection amplitude of the tip of the Euler-Bernoulli beam under unit harmonic point load at the free end. The response is obtained with 10,000 random samples and for $\sigma_a = \{0.05, 0.20\}$. The response for different order of spectral functions is shown. For this problem the degrees of freedom $n=200$ and the number of random variables $M=2$. The proposed Galerkin approach needs solution of a 10×10 linear system of equations only. (a) Beam deflection for $\sigma_a = 0.05$. (b) Beam deflection for $\sigma_a = 0.2$.

has also been mentioned in discussion of spectral functions in Section 3.3.

Fig. 6 shows the standard deviation of the frequency domain response of the tip deflection for different spectral orders of solution of the reduced basis approach and is compared with the direct MCS and 4th order PC for different values of σ_a. We find that the standard deviation is maximum at the resonance frequencies which is consistent with Fig. 4. It is again observed that the direct MCS solution and the reduced order approach give almost identical results, which demonstrate the effectiveness of the proposed approach. The 4th order PC results however, show significant inconsistencies for higher values of σ_a and especially at high frequencies. Both these observations suggest that the PC expansion of a similar order to this proposed spectral function approach may not be well suited to handle the dynamic problem at high frequencies and for high degrees of variability of the random field involved.

It can also be considered that the system response constructed with the first order spectral functions corresponds to a zeroth order expansion in the classical Neumann scheme. Thus, it would correspond to the deterministic system response shown in Figs. 4 and 6. It can be seen that the response with the first order spectral functions on the other hand gives a better approximation of the solution even at high values of standard deviation of the random field. This is a significant advantage of the proposed method over the classical Neumann expansion technique, and the results obtained with the latter is given later in this section.

Fig. 7 shows the standard deviation of the response of the beam at four different frequencies, 50 Hz, 168 Hz, 246 Hz and 418 Hz, as a function of the standard deviation of the random field. 180 Hz and 418 Hz correspond to the resonance frequencies of the cantilever beam, while 246 Hz corresponds to the anti-resonance frequency.

The relative standard deviation values have been obtained for a set of 4 values of σ_a, which represents the different degrees of variability of the system parameters. The results obtained with the Galerkin approach for the different order of spectral functions have been compared with the direct MCS, and a good agreement is observed. However, the 4th order PC result points to the fact that at high frequencies and for high values of the variance of the random field, the PC results provide a less accurate prediction of the solution moments for the same order of expansion of the polynomials of the random variables. It may be pointed out that the standard deviation decreases with the values of σ_a for the resonance frequency while it increases for the anti-resonance frequencies. This is once again consistent with the results shown in Fig. 4 which shows that an increased value of the variance of the random field has the effect of an enhanced system damping when plotting the mean value of the frequency response.

The probability density function of the deflection of the tip of the cantilever beam for different degrees of variability of the random field is shown in Fig. 8. The probability density functions

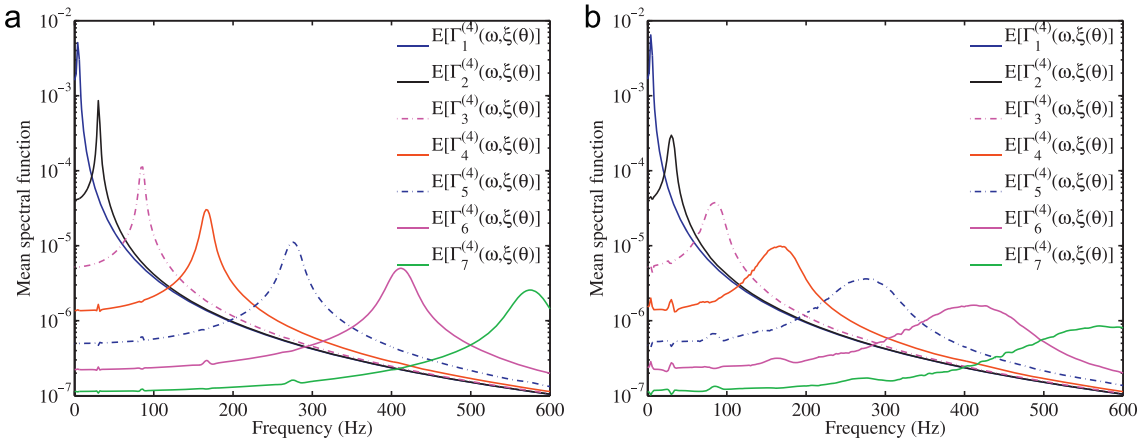

Fig. 5. The mean of the amplitude of the first seven spectral functions of order 4. The spectral functions are obtained for frequency up to 600 Hz with 10,000 sample MCS and for $\sigma_a = \{0.05, 0.20\}$. (a) Mean spectral functions for $\sigma_a = 0.05$. (b) Mean spectral functions for $\sigma_a = 0.2$.

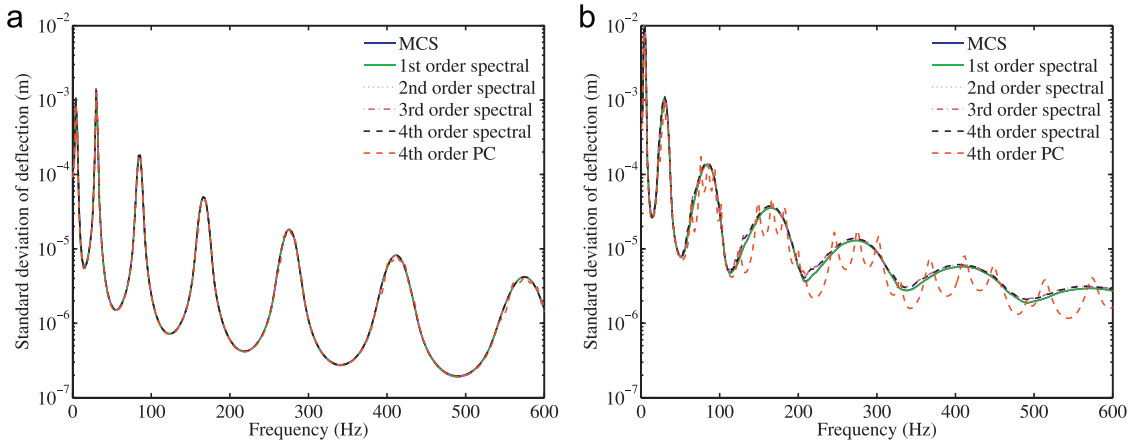

Fig. 6. The standard deviation of the deflection amplitude of the tip of the Euler–Bernoulli beam under unit harmonic point load at the free end. The response is obtained with 10,000 random samples and for $\sigma_a = \{0.05, 0.20\}$. (a) Standard deviation of the response for $\sigma_a = 0.05$. (b) Standard deviation of the response for $\sigma_a = 0.2$.

have been calculated at the frequency of 418 Hz, which is a resonance frequency of the beam.

A close match between the direct MCS and the reduced basis spectral solution is obtained. However, the density functions obtained with 4th order PC show inconsistencies, and the disparity increases with higher values of σ_a. These results establish the applicability of this spectral reduced basis method with Galerkin error minimization technique as a satisfactory working model for providing solution of the stochastic dynamical systems. The method is found to be consistent with the direct MCS approach, while being computationally efficient than either the direct MCS or PC approach. For a given order of expansion, the proposed method approximates the stochastic system response better than the classical Neumann expansion.

Here we highlight the behavior of an error norm of the system response obtained with this spectral function approach for different orders of the spectral functions, the application of the Galerkin technique and for different degrees of variability of the parametric uncertainty. Hence we consider a L^2 relative error for the mean response of the cantilever beam. The L^2 relative error $\epsilon_{\mu}^{(m)}(\omega)$ is defined at each frequency step ω for mth order spectral functions as

$$\epsilon_{\mu}^{(m)}(\omega) = \frac{\left\| \boldsymbol{\mu}_{SF}^{(m)}(\omega) - \boldsymbol{\mu}_{MCS}(\omega) \right\|_{L^2(\mathcal{D})}}{\left\| \boldsymbol{\mu}_{MCS}(\omega) \right\|_{L^2(\mathcal{D})}} \tag{45}$$

where $\boldsymbol{\mu}_{SF}^{(m)}(\omega)$ denotes the mean of the response vector obtained with the stochastic spectral functions of order m and $\boldsymbol{\mu}_{MCS}(\omega)$ is the mean response vector calculated with the direct MCS simulation. Here we have studied the cases for which $m = 1, \ldots, 4$ and present the convergence of the L^2 relative error with increasing order of the spectral functions. Now, errors induced in the system due to the reduced number of basis functions and finite order of the spectral functions induces error in the computational scheme which has been minimized with the Galerkin-type error orthogonalization technique as presented in Section 4.2. Hence we present here the mean response calculated before and after the application of the Galerkin technique in order to demonstrate the effectiveness of the latter in approximating the solution for lower orders of the spectral functions and fewer modal basis vectors.

Fig. 9(a) shows the behavior of the L^2 relative error as a function of frequency for the 2nd order spectral functions with and without the application of the Galerkin type orthogonalization of the residual vector to the modal basis.

It can be seen that for the Galerkin method consistently reduces the L^2 error at almost all frequencies, but performs better in the low frequency range. Also, the overall error tends to increase with frequency which is expected since the contribution of the higher order modes becomes significant at these frequencies and the truncation error grows. The standard deviation value has been chosen as $\sigma_a = 0.20$ which represents quite a high variability of the random field. Fig. 9(b) shows a comparison of the L^2 error obtained with the 1st and 4th order spectral functions for $\sigma_a = 0.20$ and proves that increasing the spectral function order improves the

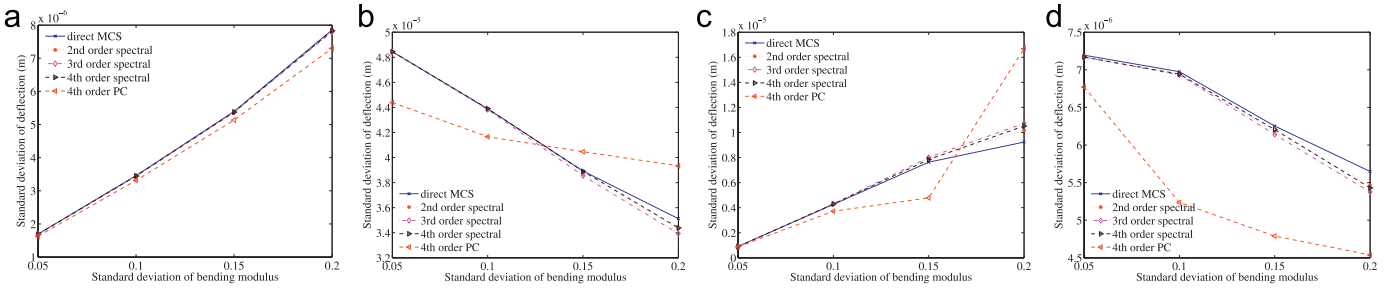

Fig. 7. Standard deviation of the deflection amplitude of the tip of the Euler–Bernoulli beam for different degrees of parametric uncertainty represented by $\sigma_a = \{0.05, 0.10, 0.15, 0.20\}$ at 4 different frequencies and under unit harmonic point load at the free end. The response is obtained with 10,000 random samples. Note that 168 and 418 Hz correspond to the resonance frequencies of the beam. (a) Standard deviation of the response at 50 Hz. (b) Standard deviation of the response at 168 Hz. (c) Standard deviation of the response at 246 Hz. (d) Standard deviation of the response at 418 Hz.

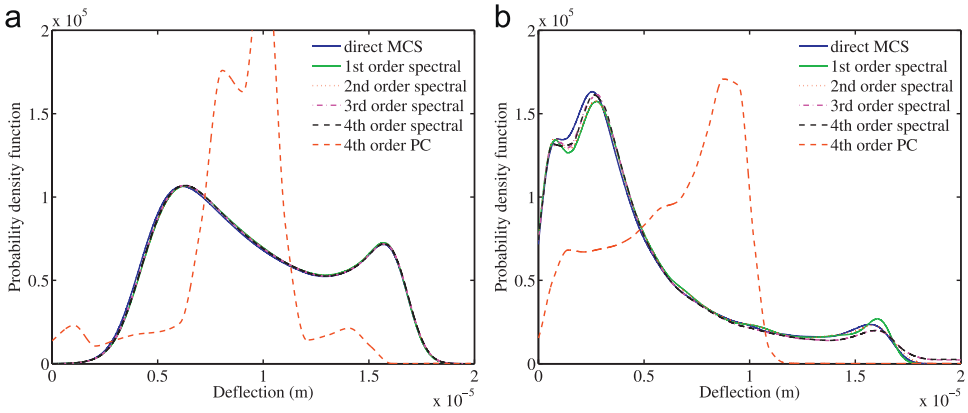

Fig. 8. The probability density function of the deflection amplitude of the tip of the cantilever beam under a unit harmonic point load at the free end at 418 Hz. The pdfs are obtained with 10,000 random samples and for two values of $\sigma_a = \{0.05, 0.20\}$. (a) Probability density function for $\sigma_a = 0.05$. (b) Probability density function for $\sigma_a = 0.2$.

results quite well at low frequencies. However, beyond 400 Hz, it is less effective, which can be explained as follows: at high frequencies, the overall error level increases (as is indicated by the increasing trend of the curve) which implies that the modal truncation, performed in obtaining the solution in the reduced space, results in the elimination of the contribution of some higher order modes which may be significant at these frequencies.

To study the convergence behavior of the response approximated with different orders of the spectral functions, we look at the mean squared error of the response at particular frequencies as a function of the spectral function order in Fig. 10 for different values of standard deviation of the underlying random parameter.

It is found that the Galerkin error reduction is quite effective for lower (1st and 2nd) order of spectral functions, however, for solutions approximated with higher order spectral functions, the application of the Galerkin scheme has no appreciable effect on the response.

Fig. 11 shows the comparison of the results obtained with the spectral function approach with that of the classical Neumann expansion technique. It can be seen from Fig. 11(a) that near the resonance frequencies the Neumann expansion solution does not converge. Fig. 11(b) and (c) shows a comparison between the relative L^2 error of the system response obtained with the 4th order spectral functions and different orders of expansion of the Neumann method for two different values of standard deviation of the parametric uncertainty, $\sigma_a = 0.05, 0.20$. It shows that while at non-resonant frequencies, the error values are identical to those predicted by the spectral function approach, they deteriorate significantly in the neighborhood of the resonance frequencies. The effect is more significant for high values of standard deviation, (like $\sigma_a = 0.20$), where the solution has been rendered meaningless over the entire frequency spectrum. It must be mentioned that the damping values chosen for the simulation has a significant effect on the Neumann expansion technique, and the radius of convergence increases for high damping.

Thus, the spectral function approach proposed here is found to provide accurate values of the system response at low computational cost (verified against the direct MCS results) over a wide range of frequencies, and quite high values of standard deviation of the random parameter of the stochastic structural system. Even a comparison with the polynomial chaos method shows that the latter requires the use of higher order stochastic basis functions for providing a good approximation of the solution near the resonance frequencies and especially for high values of standard deviation of the random field σ_a. However, the added computational cost associated with this p-refinement is substantial. The spectral function approach proposed here uses a rational form of the polynomials of the random variables to approximate the solution in the stochastic space. This provides a better approximation of the system response even with lower order functions.

6.2. Case II: Kirchhoff–Love plate

In this section we apply the proposed spectral method to a Kirchhoff–Love plate clamped at one edge (where the displacement and the rotational degrees of freedom are set to zero). For the present case we have assumed the bending stiffness to be the stochastic parameter of the plate. The damping model chosen for

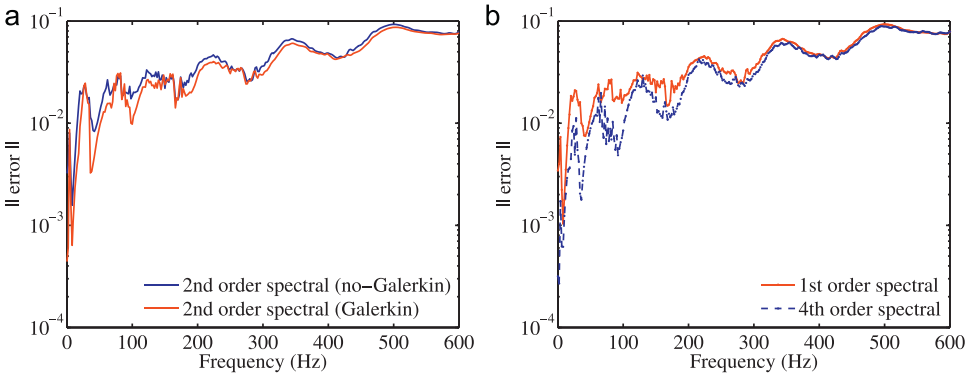

Fig. 9. (a) The L^2 relative error of the response obtained with the 2nd order spectral functions with and without the Galerkin type error minimization for the parametric standard deviation of $\sigma_a = 0.20$ (b) Comparison of the L^2 error of the response obtained using 1st and 4th order spectral functions in conjunction with the Galerkin type error minimization for the parametric standard deviation of $\sigma_a = 0.20$. (a) L^2 error for 2nd order spectral functions. (b) Comparison ofL^2 error with 1st and 4th order spectral functions.

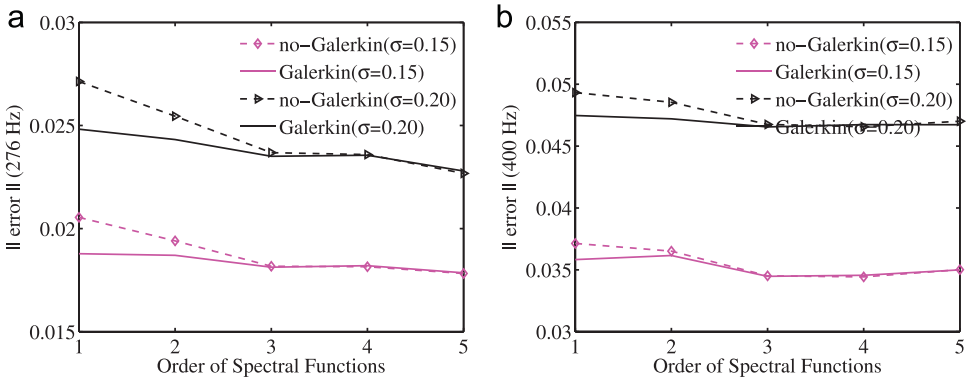

Fig. 10. Convergence of the L^2 error of the response vector at 276 Hz (resonance frequency) and 400 Hz with increasing order of spectral functions for the random parameter for two different values of standard deviation $\sigma_a = \{0.15, 0.20\}$. (a) L^2 error at 276 Hz. (b) L^2 error at 400 Hz.

this case is that of constant modal damping, with 1% damping factor for all the modes. Fig. 12(a) shows the configuration of the rectangular plate in a deformed configuration with a harmonic point load on one of its free corners. The origin of the global coordinate system is assumed to be at the centre of the rectangular plate. We assume that the bending modulus is a stationary Gaussian random field of the form:

$$D(x, y, \theta) = D_0(1 + \epsilon(x, y, \theta)) \tag{46}$$

where x and y are the coordinate direction along the length and width of the plate respectively, D_0 is the baseline modulus of elasticity, $\epsilon(x, y, \theta)$ is a zero mean stationary Gaussian random field. The autocorrelation function of this random field is assumed to be of the form:

$$C_a(x_1, x_2; y_1, y_2) = \sigma_a^2 e^{-(|x_1-x_2|)/\mu_x} e^{-(|y_1-y_2|)/\mu_y} \tag{47}$$

where μ_x and μ_y are the correlation lengths along the x and y coordinate axes respectively, and σ_a is the standard deviation of the elastic modulus. We use the base-line parameters as the length $L_x = 1$ m, width $L_y = 0.6$ m, thickness $t = 3$ mm, mass density $\rho = 7860$ kg/m^3, Poisson ratio $\mu = 0.3$ and mean elastic modulus $D_0 = 2 \times 10^{11}$ Pa. For the finite element discretization, the beam is divided into 32 elements along its length (x direction) and 18 elements along its width (y direction). Standard 12 degree of freedom Kirchhoff plate elements are used for the finite element modeling. The total number of degrees of freedom of the plate system after the application of the boundary conditions come to 1881. The correlation length is taken as 1/5th of the plate dimension along both the x and y directions, thus $\mu_x = L_x/5$ and $\mu_y = L_y/5$. The KL series expansion presented in Eq. (8) is truncated at 4 terms along the orthogonal coordinate axes and using the tensor product of these eigen functions we have a total of 16 random variables to represent the discretized the random elastic modulus in the spatial domain. Therefore, for this problem we have $n = 1881$ and $M = 16$. The vibration response have been obtained for two different values of the standard deviation of the random field, $\sigma_a = \{0.05, 0.15\}$. The external forcing vector is taken to be deterministic and having a unit norm. The dynamic vibration response of the plate under the action of a point load acting at one of its free corners is now presented. The response is measured at the node under loading for different values of the random field variability, σ_a. The frequency range of interest is 0–500 Hz at an interval of 5 Hz. The reduced spectral method simulation and the reduced basis direct MCS simulation have been performed with 10,000 random samples.

Fig. 12(a) shows the mean deformation shape of the plate under the prescribed loading condition at 300 Hz. Fig. 12(b) shows the distribution of the natural frequencies of the plate calculated with the deterministic system matrices. The chosen reduced number of eigenvectors (150) for the problem is marked in the figure, which approximately covers up to 2000 Hz, which is about 4 times the maximum frequency of the problem (500 Hz). Thus the Galerkin method requires the solution of a 150×150 system of linear equations in order to evaluate the constants associated with the stochastic basis. In contrast, for the PC solution technique using 4th order polynomial functions, calculations reveal that it is necessary to solve a $9{,}113{,}445 \times 9{,}113{,}445$ dimensional linear system of equations in order to obtain the undetermined coefficients for every frequency point, which incurs a substantial computational cost. It must be noted though, that the linear system obtained after orthogonalizing the residual to the stochastic solution subspace is a large block sparse system and the solution can potentially be speeded up with iterative Krylov-based linear solvers

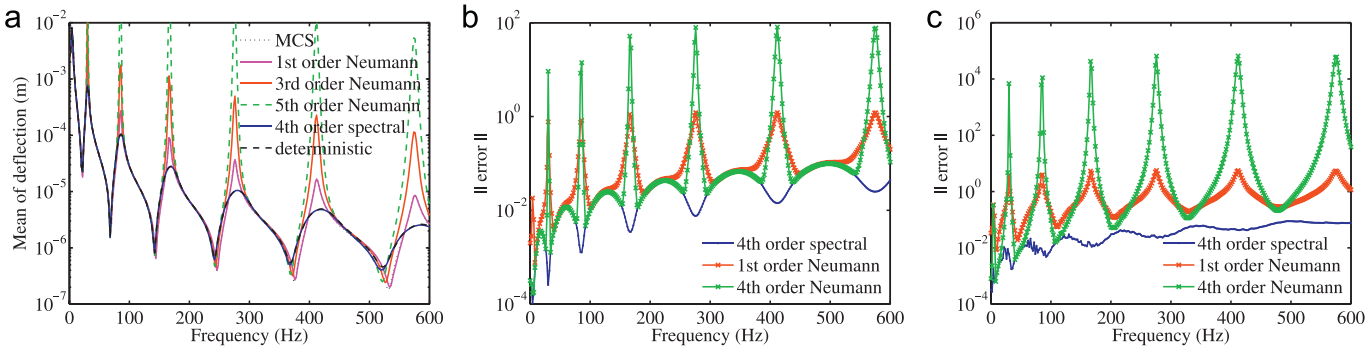

Fig. 11. (a) Stochastic system response calculated using different orders of Neumann expansion and compared to the direct MCS results for $\sigma_a = 0.10$. (b) Comparison of the L^2 relative error of the response vector obtained with the Neumann expansion and the spectral function approach for standard deviation $\sigma_a = 0.05$ (c) Comparison of the L^2 relative error of the response vector obtained with the Neumann expansion and the spectral function approach for standard deviation $\sigma_a = 0.20$. (a) Beam deflection for $\sigma_a = 0.10$. (b) L^2 error for $\sigma_a = 0.05$. (c) L^2 error for $\sigma_a = 0.20$.

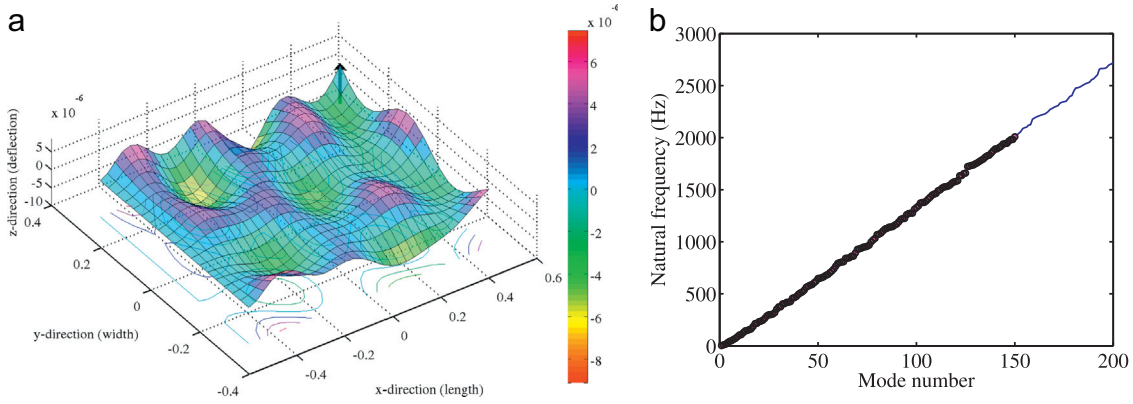

Fig. 12. (a) Dynamic plate vibration shape at 300 Hz with a harmonic point force at one of the free corners. The plate is clamped at one of its edges ($x = -0.5$). The plate is loaded at one of the free corners ($x=0.5$, $y=0.3$). (b) Natural frequency distribution of the vibrating plate highlighting the first 150 natural frequencies. (a) Plate vibration shape at 300 Hz. (b) Natural frequency distribution.

and appropriate preconditioners [22]. If the PC expansion is applied to the dynamic system in its modal coordinates with the solution being projected on the first 150 eigenmodes, then it would be necessary to solve a block sparse linear system of dimension $726{,}750 \times 726{,}750$. However, now each 150×150 block of the 726,750-dimensional sparse coefficient matrix would be a dense matrix.

Fig. 13 shows the frequency domain response of the mean deflection of the Kirchhoff–Love plate obtained with different orders of spectral functions (1st, 2nd, 3rd and 4th) and has been compared with the direct MCS results and the deterministic system response. It is observed that the response obtained with the spectral method matches the direct MCS results quite closely. For higher values of σ_a we find the mean response to attenuate with frequency, which is similar to the case of beam bending problem in the previous section.

The plots in Fig. 14 show the standard deviation of the stochastic system response over the frequency range. Once again, the spectral function approach produces agreeable results with the direct MCS simulation. The approximation of the different moments of the response with varying orders of the spectral functions is of particular interest to this study. The L^2 relative error norm described in Eq. (45) would be of particular interest in this context, which is presented later in the section

Now we look into the relative L^2 error characteristics defined in Eq. (45). Fig. 15 shows effectiveness of using the Galerkin technique in terms of improving the relative L^2 error of the mean deflection calculated with the 1st and 5th order spectral functions. It is seen that the Galerkin type error minimization has a significant effect on the solution approximated with the 1st order spectral functions at almost all frequencies (Fig. 15(a)). Thus, the Galerkin technique takes care of the modal contributions by adjusting the values of the undetermined coefficients $c_k(\omega)$, $k = 1, 2, \ldots, n_r$ where n_r is the dimension of the reduced system. However, the solution obtained with the 5th order spectral functions, given in Fig. 15(b), shows little effect of the application of the Galerkin method. This indicates that the solutions have already been approximated to a sufficient degree of accuracy using the higher order terms in the spectral functions and the modal coupling of the vibrating system in approximating the response is already quite high. Also, it can be seen that the overall relative error levels are reduced when we use the 5th order spectral functions to approximate the solution, especially beyond the low frequency region (say 100 Hz).

The improvement in the overall relative L^2 error at all frequencies is demonstrated in Fig. 16, which shows that the error calculated with the mean deflection values obtained with 2nd and 5th order spectral functions in conjunction with the Galerkin method for different values of variability of the parametric randomness (indicated by σ_a). There is a good improvement in the results with the 5th order functions, except for the low frequency region (below 100 Hz) and for low value of σ_a. For a higher value of standard deviation of the

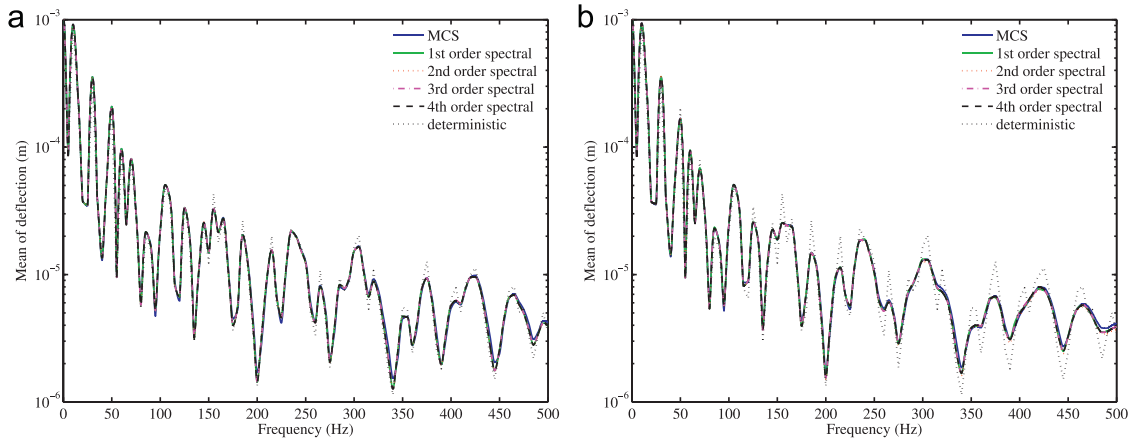

Fig. 13. The mean of the deflection amplitude of a free corner of a Kirchhoff–Love thin plate under a unit harmonic point load. The response is obtained with 10,000 random samples and for $\sigma_a = \{0.05, 0.10\}$. The response for different order of spectral functions are shown. For this problem the degrees of freedom $n=1881$ and the number of random variables $M=16$. The proposed Galerkin approach needs solution of a 150×150 linear system of equations. (a) Plate deflection for $\sigma_a = 0.05$. (b) Plate deflection for $\sigma_a = 0.1$.

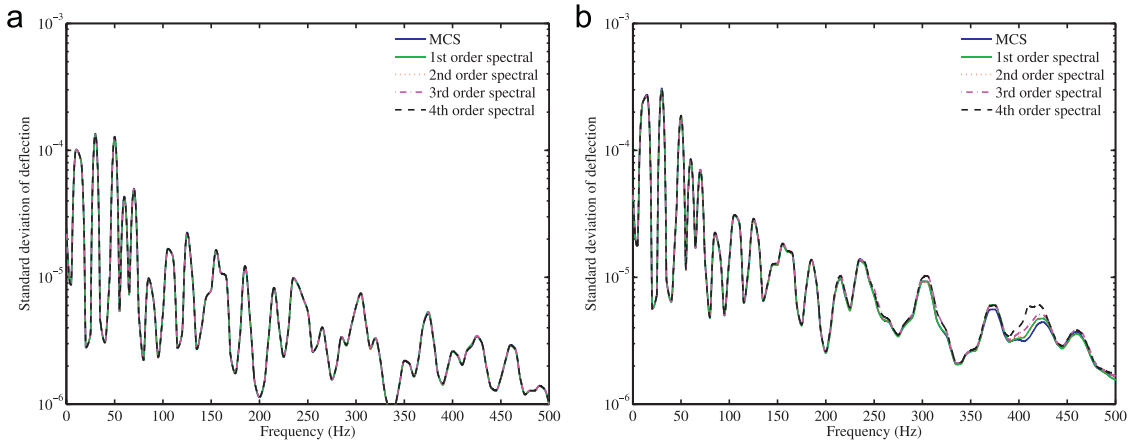

Fig. 14. The standard deviation of the deflection amplitude of a free corner of a Kirchhoff–Love thin plate under a unit harmonic point load. The response is obtained with 10,000 random samples and for $\sigma_a = \{0.05, 0.10\}$. (a) Standard deviation of the response for $\sigma_a = 0.05$. (b) Standard deviation of the response for $\sigma_a = 0.1$.

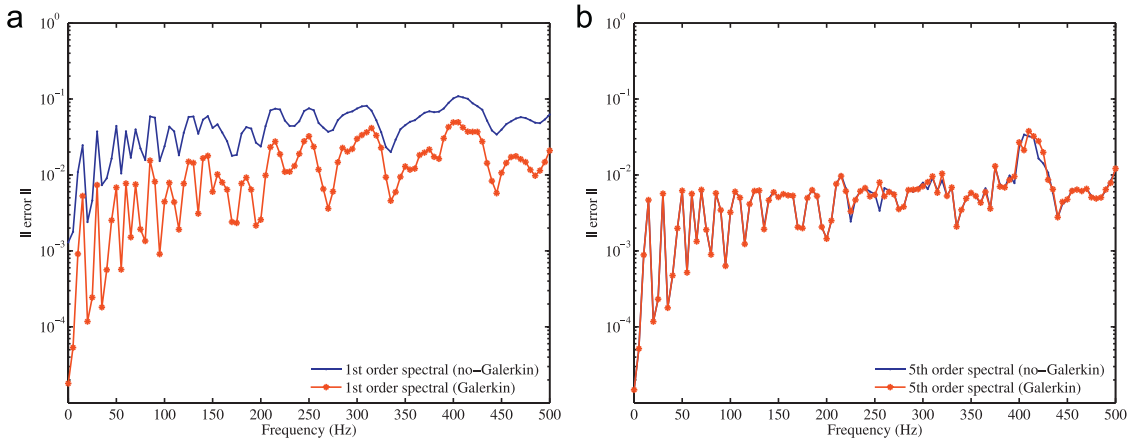

Fig. 15. The relative L^2 error of the mean deflection of the Kirchhoff–Love thin plate under a unit harmonic point load. The response has been approximated with 1st and 5th order spectral functions and the error is studied before and after the application of the Galerkin scheme. Simulations have been performed with 10,000 random samples and for standard deviation of $\sigma_a = 0.10$ of the random parameter. (a) L^2 error with 1st order spectral functions. (b) L^2 error with 5th order spectral functions.

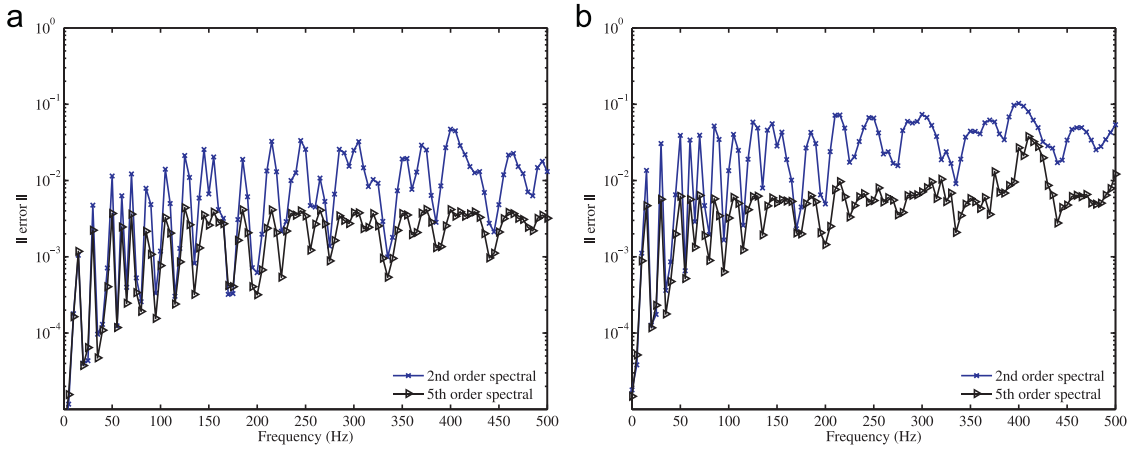

Fig. 16. The relative L^2 error of the mean deflection of the Kirchhoff–Love thin plate under a unit harmonic point load obtained with 2nd and 5th order spectral functions. Simulations have been performed with 5000 random samples and for standard deviation of $\sigma_a = 0.05$ and $\sigma_a = 0.10$ of the random parameter. (a) L^2 error for $\sigma_a = 0.05$. (b) L^2 error for $\sigma_a = 0.10$.

random field ($\sigma_a = 0.10$), the improvement in results with the higher order spectral functions is more than that for $\sigma_a = 0.05$. Thus, implies that the higher order spectral functions are more useful for high values of standard deviation of the random field.

Finally, Fig. 17 demonstrates the effect of increasing the order spectral functions on the L^2 relative error of the solution. The behavior is shown at particular values of frequencies, to clearly identify the solution traits. The frequencies are chosen such that the use of higher order functions improve the results significantly at those points. The curves show that the Galerkin method has a significant role in reducing the error of the solution obtained with 1st and 2nd order spectral functions, and little effect on those with higher orders. It is observed at all the frequencies that a significant improvement in the results is obtained as we move from the 2nd

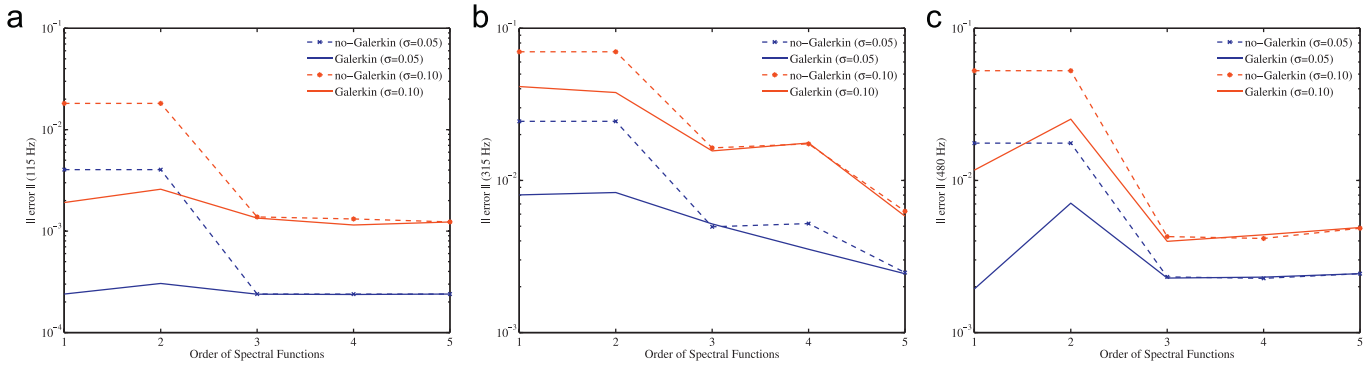

Fig. 17. The relative L^2 error of the mean deflection of the Kirchhoff–Love thin plate under a unit harmonic point load with increasing order of spectral functions at 110, 315 and 480 Hz. Simulations have been performed with 10,000 random samples and for standard deviation of $\sigma_a = \{0.05, 0.10\}$ of the random parameter. (a) L^2 error at 115 Hz. (b) L^2 error at 310 Hz. (c) L^2 error at 480 Hz.

to the 3rd order values when the Galerkin technique is not being used. The application of the Galerkin error minimization technique brings down the error values close to those obtained normally (without the Galerkin) with the higher order (4 and 5) spectral functions. It can also be seen, especially in Fig. 17(c), that the Galerkin technique reduces the 1st order error to a lower value than that with the second order spectral function. Also, while the higher order functions almost always provides a better solution accuracy yet, the higher order functions must be used prudently. An identifiable trend of the L^2 error with increasing spectral function order has not been observed in the results presented here, and hence the extent of this kind of 'p-refinement' (by increasing the order of spectral functions) may not be obvious. Investigation into some optimality criterion which can provide some adaptivity in terms of the optimum order of the spectral functions and the dimension of the reduced modal basis of the problem would be quite helpful to minimize the computational cost in these kind of problems.

7. Conclusions

We have considered the stochastic partial differential equation for structural dynamic systems with generally non-Gaussian random fields. The stochastic system response is resolved using a set of complex, frequency-adaptive, rational stochastic weighting functions, called the spectral functions. A Galerkin-type error minimization approach has been proposed which uses a set of frequency dependent undetermined coefficients to orthogonalize the residual to the reduced modal subspace. The proposed solution technique has been used to solve two stochastic dynamic problems – an Euler–Bernoulli cantilever beam and another Kirchhoff–Love thin plate subjected to harmonic forcing over a frequency range. The results obtained with the spectral function approach is in good agreement with the direct MCS simulation at all frequencies and different degrees of input variability. The proposed methodology shows good solution accuracy compared to what is obtained with polynomial basis functions or the Neumann expansion technique. This is attributed to the rational functional form of the spectral functions which improves their convergence radius even near the resonance frequencies even when for low order expansions. The results demonstrate the applicability and computational efficacy of the stochastic spectral function approach proposed in this work.

Future work along this direction may be aimed at reducing the computational burden of integration over the probability space using the efficient variance reduction and/or sampling techniques. The choice of the optimum order of spectral functions and the dimension of the reduced modal subspace can be made adaptive which requires further investigation. Further research on a-priori error analysis can also give important intuitive guidance in moving towards a choice of a more efficient set of basis functions suitable for this class of stochastic structural dynamic problems.

Acknowledgments

A.K. acknowledges the financial support from the Swansea University through the award of the Zienkiewicz scholarship. S.A. acknowledges the financial support from The Royal Society of London through the Wolfson Research Merit Award.

References

[1] A. Nouy, Recent developments in spectral stochastic methods for the numerical solution of stochastic partial differential equations, Arch. Comput. Methods Eng. 16 (3) (2009) 251–285.
[2] D.C. Charmpis, G.I. Schuëller, M.F. Pellissetti, The need for linking micromechanics of materials with stochastic finite elements: a challenge for materials science, Comput. Mater. Sci. 41 (1) (2007) 27–37.
[3] G. Stefanou, The stochastic finite element method: past, present and future, Comput. Methods Appl. Mech. Eng. 198 (9–12) (2009) 1031–1051.
[4] H.J. Pradlwarter, G.I. Schuëller, On advanced monte carlo simulation procedures in stochastic structural dynamics, Int. J. Non-Linear Mech. 32 (4) (1997) 735–744 (Third International Stochastic Structural Dynamics Conference).
[5] F. Yamazaki, M. Shinozuka, Digital generation of non-Gaussian stochastic fields, J. Eng. Mech. 114 (7) (1988) 1183–1197.
[6] G. Falsone, G. Ferro, A method for the dynamical analysis of FE discretized uncertain structures in the frequency domain, Comput. Methods Appl. Mech. Eng. 194 (42–44) (2005) 4544–4564.
[7] M. Kleiber, T.D. Hien, The Stochastic Finite Element Method, John Wiley, 1992.
[8] F. Yamazaki, M. Shinozuka, G. Dasgupta, Neumann expansion for stochastic finite element analysis, J. Eng. Mech.—ASCE 114 (8) (1988) 1335–1354.
[9] W.Q. Zhu, Y.J. Ren, W.Q. Wu, Stochastic FEM based on local averages of random vector fields, J. Eng. Mech. 118 (3) (1992) 496–511.
[10] M.K. Deb, I.M. Babuska, J.T. Oden, Solution of stochastic partial differential equations using galerkin finite element techniques, Comput. Methods Appl. Mech. Eng. 190 (48) (2001) 6359–6372.
[11] I. Babuska, R. Tempone, G.E. Zouraris, Solving elliptic boundary value problems with uncertain coefficients by the finite element method: the stochastic formulation, Comput. Methods Appl. Mech. Eng. 194 (12–16) (2005) 1251–1294.
[12] H.G. Matthies, A. Keese, Galerkin methods for linear and nonlinear elliptic stochastic partial differential equations, Comput. Methods Appl. Mech. Eng. 194 (12–16) (2005) 1295–1331.
[13] R.G. Ghanem, R.M. Kruger, Numerical solution of spectral stochastic finite element systems, Comput. Methods Appl. Mech. Eng. 129 (3) (1996) 289–303.
[14] A. Keese, H.G. Matthies, Hierarchical parallelisation for the solution of stochastic finite element equations, Comput. Struct. 83 (14) (2005) 1033–1047.
[15] H.G. Matthies, C.E. Brenner, C.G. Bucher, C.G. Soares, Uncertainties in probabilistic numerical analysis of structures and solids - stochastic finite

elements, Struct. Saf. 19 (3) (1997) 283–336.
[16] P. Spanos, M. Beer, J. Red-Horse, Karhunen–Loève expansion of stochastic processes with a modified exponential covariance kernel, J. Eng. Mech. 133 (7) (2007) 773–779.
[17] D.B. Xiu, G.E. Karniadakis, The Wiener–Askey polynomial chaos for stochastic differential equations, SIAM J. Sci. Comput. 24 (2) (2002) 619–644.
[18] A. Sarkar, R. Ghanem, Mid-frequency structural dynamics with parameter uncertainty, Comput. Methods Appl. Mech. Eng. 191 (47–48) (2002) 5499–5513.
[19] R. Ghanem, P.D. Spanos, Stochastic Finite Elements: A Spectral Approach, Springer-Verlag, New York, USA, 1991.
[20] S. Adhikari, Stochastic finite element analysis using a reduced orthonormal vector basis, Comput. Methods Appl. Mech. Eng. 200 (21–22) (2011) 1804–1821.
[21] A. Kundu, F. DiazDelaO, S. Adhikari, M. Friswell, A hybrid spectral and meta-modeling approach for the stochastic finite element analysis of structural dynamic systems, Comput. Methods Appl. Mech. Eng. 270 (0) (2014) 201–219.
[22] Y. Saad, Iterative Methods for Sparse Linear Systems, Society for Industrial and Applied Mathematics, 2003.